EBioMedicine 2 (2015) 1785–1798

Contents lists available at ScienceDirect

EBioMedicine

journal homepage: www.ebiomedicine.com

Research Article

Stress Granules Modulate SYK to Cause Microglial Cell Dysfunction in Alzheimer's Disease

Soumitra Ghosh, Robert L. Geahlen *

Department of Medicinal Chemistry and Molecular Pharmacology, Purdue University, West Lafayette, IN 47907, USA

ARTICLE INFO

Article history:
Received 13 August 2015
Received in revised form 21 September 2015
Accepted 30 September 2015
Available online 3 October 2015

Keywords:
Alzheimer's disease
Microglial cells
Stress granules
SYK tyrosine kinase
Neurodegenerative disease
Amyloid-beta

ABSTRACT

Microglial cells in the brains of Alzheimer's patients are known to be recruited to amyloid-beta (Aβ) plaques where they exhibit an activated phenotype, but are defective for plaque removal by phagocytosis. In this study, we show that microglia stressed by exposure to sodium arsenite or Aβ(1–42) peptides or fibrils form extensive stress granules (SGs) to which the tyrosine kinase, SYK, is recruited. SYK enhances the formation of SGs, is active within the resulting SGs and stimulates the production of reactive oxygen and nitrogen species that are toxic to neuronal cells. This sequestration of SYK inhibits the ability of microglial cells to phagocytose *Escherichia coli* or Aβ fibrils. We find that aged microglial cells are more susceptible to the formation of SGs; and SGs containing SYK and phosphotyrosine are prevalent in the brains of patients with severe Alzheimer's disease. Phagocytic activity can be restored to stressed microglial cells by treatment with IgG, suggesting a mechanism to explain the therapeutic efficacy of intravenous IgG. These studies describe a mechanism by which stress, including exposure to Aβ, compromises the function of microglial cells in Alzheimer's disease and suggest approaches to restore activity to dysfunctional microglial cells.

1. Introduction

Microglial cells (MG) are the professional macrophages of the central nervous system. Among their many tasks is the removal from the brain of aggregates of amyloid-beta (Aβ), which is formed from a proteolytic product of amyloid precursor protein (Huang and Mucke, 2012). The persistent accumulation of Aβ plaques is a characteristic of Alzheimer's disease (AD), a serious neurodegenerative disorder affecting millions of patients worldwide. MG are attracted to sites of Aβ deposition, which they recognize through a variety of cell surface receptors, and are capable of Aβ removal through phagocytosis (Solito and Sastre, 2012; Gandy and Heppner, 2013). Impaired microglial activity, as exhibited by defective removal of Aβ plaques, is particularly associated with the later stages of AD as plaques accumulate (Krabbe et al., 2013; Hickman et al., 2008; Mosher and Wyss-Coray, 2014). These plaques still attract MG, but are refractory to phagocytosis. While MG can phagocytose Aβ fibrils, they also become activated as a consequence of receptor engagement by Aβ (Meyer-Luehmann et al., 2008; Jekabsone et al., 2006; Bianca et al., 1999). The activation of MG is problematic as the resulting inflammatory response can damage neighboring neuronal cells (Bianca et al., 1999). Compelling evidence for an important role of MG in AD comes, in part, from large scale studies of genes associated with AD that directly implicate inflammatory responses of MG as critical for AD pathology. Products of genes with identified associations with AD include TREM2, TYROBP and CD33 (Guerreiro et al., 2013; Jonsson et al., 2013; Bertram et al., 2008; Hollingworth et al., 2011; Naj et al., 2011; Zhang et al., 2013). The myeloid receptor TREM2 functionally associates with TYROBP and promotes the internalization of bacteria and apoptotic neurons and recruits MG to Aβ plaques (N'Diaye et al., 2009; Takahashi et al., 2005, Wang et al., 2015; Jay et al., 2015). Loss-of-function mutants promote inflammatory responses, decrease phagocytosis and predispose patients to AD (Guerreiro et al., 2013). CD33 is upregulated in MG in AD brain and is associated with reduced uptake of Aβ and increased numbers of activated, pro-inflammatory MG (Griciuc et al., 2013).

Many phagocytic receptors contain or are associated with proteins such as TYROBP that contain immunoreceptor tyrosine-based activation motifs (ITAMs) (Linnartz et al., 2010; Cambier, 1995). Receptor engagement initiates the phosphorylation of the two ITAM tyrosines leading to a physical interaction with the tyrosine kinase, SYK (Geahlen, 2009). Signaling through ITAM receptors is attenuated by receptors with immunoreceptor tyrosine-based inhibitory motifs (ITIMs) such as CD33 (Angata et al., 2002). Since SYK is essential for both phagocytosis in macrophages and for the receptor-mediated activation of

Abbreviations: Aβ, amyloid-beta; AD, Alzheimer's disease; IgG, immunoglobulin G; MG, microglial cells.

* Corresponding author at: Department of Medicinal Chemistry and Molecular Pharmacology, Hansen Life Sciences Research Building, 201 S. University St., West Lafayette, IN 47907, USA.
E-mail address: geahlen@purdue.edu (R.L. Geahlen).

http://dx.doi.org/10.1016/j.ebiom.2015.09.053

inflammatory responses (Kiefer et al., 1998; Crowley et al., 1997), two events that are disrupted in MG from AD brains, it would appear to be a prime candidate for a critical mediator of AD pathology. An important question is how the function of SYK might be disrupted in aged or stressed MG.

MG in aged and AD brain fail to clear Aβ plaques, but display an activated, pro-inflammatory phenotype (Krabbe et al., 2013; Hickman et al., 2008; Mosher and Wyss-Coray, 2014). How aging and other stresses affect MG to alter their homeostatic functions is unclear. Eukaryotic cells respond to external stresses via the formation of ribonucleoprotein (RNP) complexes scaffolded by RNA-binding proteins that self-associate. Examples of RNP aggregates include stress granules (SGs), which contain stalled initiation complexes and their associated mRNAs (Anderson and Kedersha, 2008; Buchan and Parker, 2009). An association of RNP aggregates with neurodegenerative diseases is well documented and mutations in RNA-binding proteins that promote self-assembly can be drivers of motor neuron diseases (Ash et al., 2014; King et al., 2012). Similarly, defective clearance of SGs leads to the pathological accumulation of RNP particles and underlies the pathology of amyotrophic lateral sclerosis, Huntington's disease, frontotemporal lobar degeneration and AD (Harris and Rubinsztein, 2011; Buchan et al., 2013; Koppers et al., 2012; King et al., 2012; Vanderweyde et al., 2012; Waelter et al., 2001; Goggin et al., 2008; Liu-Yesucevitz et al., 2010; Neumann et al., 2006; Menzies et al., 2015).

Large scale proteomic screens from our laboratory have identified multiple SG-associated proteins as binding partners and substrates for SYK (Iliuk et al., 2010; Xue et al., 2012; Galan et al., 2011). We found that SYK was recruited to SGs in MCF7 cells when exposed to sodium arsenite or proteasome inhibitors (Krisenko et al., 2015). In this study, we show that SYK also is recruited to SGs that form in MG, not only in response to sodium arsenite, but also in response to Aβ peptides or fibrils. Chronic stress leads to the formation of persistent SGs in MG in which active SYK is sequestered, leading to the constitutive production of reactive metabolites and the inhibition of phagocytic activity. Cytoplasmic aggregates containing SYK and phosphotyrosine are more pronounced in MG in the brains of patients with advanced AD. Based on this information, we propose a model in which the production of SGs and the corresponding misregulation of SYK directly contribute to AD pathology. Interestingly, the impaired phagocytic activity of stressed MG can be restored by the induced relocation of SYK from the SG to the plasma membrane by treating cells with IgG, suggesting a mechanism by which the administration of immunoglobulins to AD patients might retard disease progression.

2. Material and Methods

2.1. Cells and Cell Lines

BV-2 microglial cells developed by Blasi and colleagues (Blasi et al., 1990) were obtained from Dr. Chris Rochet (Purdue University) and cultured in DMEM media containing 10% FBS and 100 U/ml penicillin and streptomycin. N9 microglial cells (Righi et al., 1989) were obtained from Dr. Fabio Bianco (Neuro-Zone, Italy) and were cultured in ISCOVE medium containing 10% FBS and 100 U/ml penicillin and streptomycin. HEK293T cells were purchased from ATCC and HT22 neuronal cells (Davis and Maher, 1994) were obtained from Dr. Shaohua Yang, (University of North Texas). Both were grown in DMEM containing 10% FBS and 100 U/ml penicillin and streptomycin. The cDNA coding for mouse SYK-EGFP fusion protein cloned into a puromycin resistance lentiviral vector was as described (Wang et al., 2014). GIPZ mouse SYK shRNA and scrambled shRNA lentiviral plasmids were purchased from GE Dharmacon. Lentiviruses were packaged in HEK293T cells and used to infect BV-2 cells, which were then selected in puromycin.

Primary microglial cells were isolated essentially as described (Moussaud and Draheim, 2010; Lee and Tansey, 2013) from 1 month or 20 month old wild-type or $Syk^{+/-}$ C57BL/6 mice. SYK-haploinsufficient mice were generated by gene targeting by Ingenious Targeting Laboratory, Ronkonkoma, NY. The endogenous gene for Syk was replaced by a gene containing a GCA to AGC and AT to GC substitutions at nucleotides 61,527–9 and 61,568–9, respectively, and a neomycin resistance cassette 328 nucleotides upstream of exon 10. The resulting allele is not expressed resulting in a loss of SYK from homozygous animals and haploinsufficiency in heterozyotes (Supplemental Fig. 2A). Homozygous knock-out animals are not viable and die shortly after birth. Briefly, 5 mice from each group were anesthetized and perfused in the left ventricle at constant pressure for 5 min with ice cold Ringer's solution containing 2 U/ml heparin. Brains were removed and meninges separated. The brain was minced and dissociated in media containing 1 mg/ml papain, 1.2 U/ml dispase II and 20 U/ml DNase1. Cells were recovered, pipetted up and down using glass Pasteur pipettes of decreasing hole sizes, filtered through 70 μm and 40 μm cell strainers and collected in media. Cells were separated on a discontinuous percoll density gradient, collected, washed, and cultured on 1% fibronectin-coated dishes. Primary microglia were confirmed by Western blotting and immunofluorescence staining of IBA1 (Moussaud and Draheim, 2010). All mouse experiments were performed according to the guidelines of IACUC at Purdue University.

2.2. Stress Granule Formation

Cells were grown on poly-D-lysine coated cover slips in media containing 1% FBS for 12 h before treatment with sodium arsenite (SA) (1 μM), Aβ(1–42) (100 nM), or Aβ(1–42) fibrils (100 nM) for the indicated times. Aβ(1–42) (rPeptide) or Aβ(42–1) (American Peptide Company) were resuspended in DMSO, 1% NH_4OH at a concentration of 0.025 M. To prepare Aβ fibrils, DMSO soluble Aβ was sonicated for 30 min at 1 min intervals, shaken at 37 °C for 48 h and then at room temperature for 72 h (Dahlgren et al., 2002; Pan et al., 2011). Treated cells were fixed in 4% formaldehyde in PBS, permeabilized in 1% Triton X-100, blocked with 5% goat or donkey serum (depending on the species of origin of the secondary antibody) and incubated overnight at 4 °C with primary antibody diluted at a ratio of 1:1000 in 5% goat or donkey serum in PBS. Secondary antibodies Alexa Fluor 488 or 594 against mouse, rabbit, goat and donkey species were purchased from Life Technologies. Nuclei were visualized by staining with Hoeshct 33,342 (Sigma-Aldrich). Coverslips were mounted with ProLong® Gold Antifade reagent (Life Technologies) and examined using a Zeiss LSM 710 confocal microscope. Five 25× frames (average of 75 cells each frame) were randomly selected from three independent experiments and regions surrounding SGs were selected and corrected total cell fluorescence (CTCF) was calculated using ImageJ. CTCF was used to measure the SG area in arbitrary units also known as brightness values. The number of SGs was manually calculated from five random 63× frames (average of 25 cells each frame) from three independent experiments using Zeiss 2012 software. All statistical calculations were done using GraphPad Prism 6 and one-way ANOVA statistical test was performed to calculate the *P*-value. SG formation in primary cells was analyzed by two-way ANOVA. Error bars in the figures represent means ± SEM.

2.3. Western Blotting and Immunoprecipitation Assays

For general immunoblotting experiments, N9, BV-2 or primary microglial cells were lysed in buffer containing 1% NP-40, 50 mM Tris/HCl, pH 8.0, 150 mM NaCl, 5× protease inhibitor cocktail (13,911, Sigma-Aldrich), 10 μM sodium orthovandate for 15 min on ice. After centrifugation at 14,000 ×*g* for 10 min, supernatants were collected, separated by SDS-PAGE and analyzed by Western blotting. To prepare soluble and insoluble fractions, cells were lysed in buffer A (15 mM Tris–HCl, pH 7.6, 0.3 M NaCl, 15 mM $MgCl_2$, 1% Triton X-100, 10 mM Ribonucleoside Vanadyl Complex (New England Biolabs), 5× protease inhibitor cocktail and 10 μM sodium orthovanadate) on ice for 10 min. Cells were disrupted by mortar and pestle. The insoluble fraction was

isolated by centrifugation at 1500 ×*g* for 7 min and the supernatant was collected as the soluble fraction. The insoluble fraction was dissolved in SDS-sample buffer.

For immunoprecipitation assays, whole cell lysates prepared in buffer A were incubated with anti-phosphotyrosine (4G10, EMD Millipore)-coated protein G magnetic beads (Sigma-Aldrich) for 2 h at 4 °C or with GFP-Trap beads (ChromoTek) for 30 min. Beads were washed thoroughly and bound proteins eluted with SDS-sample buffer. Immune complexes were examined by Western blotting to identify associated proteins.

2.4. Microglial Cell Functional Assays

Phagocytic activity of N9 and BV-2 cells was assessed by the uptake of pHrodo™ Red *E. coli* BioParticles® (Life Technologies) or fluorescein labeled Aβ(1–42) fibrils (rPeptide). N9 and BV-2 cells were grown in poly-D-lysine coated glass bottom dishes (MatTek) for 12 h in growth media containing 1% FBS and then treated as indicated for 120 h. Cells were incubated in 2 ml Live Cell Imaging Solution (Life Technologies) with 100 μl pHrodo™ particles for 1 h in 5% CO_2 and 37 °C on a confocal microscope stage. Hoechst dye was added to visualize the nucleus. Live images of cells were taken at 30 s intervals and compiled into a video. For fixed cell images, cells incubated for 1 h were fixed and examined by confocal microscopy. Phagocytosis of fluorescent red particles was quantified by measuring the mean corrected fluorescence intensity using ImageJ software from five random equal sized frames for each treatment condition. The phagocytosis of Aβ fibrils was measured using N9 cells in a similar manner except cells were incubated for 1 h with 25 μl FITC-labeled Aβ fibrils (fibrils prepared from 0.25 M solution of soluble Aβ(1–42)). Cells were washed extensively, fixed and imaged by confocal microscopy.

Intracellular ROS production was measured using both the 5(6)-carboxy-2′,7′-dichlorodihydrofluorescein diacetate (carboxy-H2DCFDA) (Setareh Biotech) and dihydrorhodamine 123 (D123) (Life Technologies) reagents. N9 cells were grown in 96-well plates in media containing 1% FBS and treated as indicated with SA or Aβ in the presence or absence of 500 nM SYK kinase inhibitor (R406 or PRT-060318 (Selleckchem)) for 120 h. Carboxy-H2DCFDA (10 μM) was added and incubated at 37 °C for 1 h. Cells were washed 3 times with PBS. Fluorescence was measured using a microplate reader. Alternatively, treated and control cells were incubated with D123 (5 μM) for 1 h. Cells were stained with Hoechst dye, fixed and examined by confocal microscopy. Quantitative analyses used Image J to measure mean fluorescence intensity. Extracellular production of H_2O_2 was measured using Acridan Lumigen PS-3 reagents (Amersham) as described (Uy et al., 2011). Chemiluminescence was detected using a luminescence plate reader at 430 nm. N9 cells grown in media containing 1% FBS were plated on 1% fibronectin-coated 24 well plates and treated with SA, Aβ and/or SYK inhibitors for 120 h. Media was collected and reactive nitrogen species quantified by measuring nitrite levels using the Measure-iT™ High-Sensitivity Nitrite Assay Kit (Life technologies) according to manufacturer's instructions. Fluorescence was measured using a microplate reader (excitation/emission 365/450 nm).

Cytokine production was measured using the mouse ER stress ELISA strip (Signosis) according to manufacturer's instructions.

2.5. Microglia-Neuron Co-culture and Annexin V Assay

N9 microglial cells (5×10^3 cells/well) plated in poly-D-lysine-coated 24-well plates were treated as indicated with SA, Aβ and/or SYK inhibitor for 120 h. Cells were gently detached and washed with PBS. 5×10^2 cells from each treatment condition were added to an 8 μm pore size transwell insert and placed atop 1.5×10^4 HT22 cells plated in DMEM media without phenol red containing 1% FBS and 100 U/ml penicillin and streptomycin and incubated for 48 h. HT22 cells were stained with FITC Annexin V (BD Biosciences) and Hoechst dye, fixed and examined by confocal microscopy.

2.6. Human AD Clinical Samples

Paraffin-fixed human AD brain and normal brain cortex samples were obtained from the Brain and Body Donation Program, Banner Sun. Health Research Institute, Arizona (Beach et al., 2015). Samples were clinically evaluated based on several criteria including mini-mental state examination (MMSE) score, plague density, Lewy body prevalence and dementia. Paraffin fixed cortex brain slices were heated at 65 °C for 30 min, fixed with 4% paraformaldehyde, washed sequentially with different concentrations of ethanol (70%, 50%, 30%) and then subjected to antigen retrieval by heating in 10 mM Tris/HCl (pH 10) for 20 min at 85 °C. Slides were blocked with 5% donkey serum and 2% BSA overnight at 4 °C. Brain slices were stained using antibodies against SYK, IBA1, G3BP and phosphotyrosine and examined using a Zeiss 710 LSM confocal microscope.

2.7. Antibodies

The antibodies and sources used in this study were as follows: SYK (D3Z1E, Cell Signaling Technology or B01P, Abnova), phospho-SYK (Tyr525/526, 2711, Cell Signaling Technology), G3BP1 (611,126, BD Biosciences or 07–1801, EMD Millipore), pEIF2α (E90, Abcam), TIA-1(ab2712, Abcam), PABP1 (ab21060, Abcam), GFP (168AT1211, Abgent), GAPDH (6C5, Ambion), pTYR (4G10, EMD Millipore), IBA1 (ab5076, Abcam), GFAP (GF5, Abcam), TDP-43 (10,782–2-AP, Proteintech), NOS2 (ab3523, Abcam), Integrin β1 (4B7R, Santa Cruz Biotech), CD32 (ab197930, Abcam), and Rabbit IgG (Sigma-Aldrich).

3. Results

3.1. SYK Localizes to Stress Granules in Microglial Cells

Due to the small size of primary microglial cells, which makes imaging challenging, we first established the parameters for investigations at the cellular level using two established lines of cultured MG: BV-2 and N9. Immunoblotting for endogenous SYK revealed a high level of expression of SYK in both cells as shown in comparison to DG75 B cells (Fig. 1A). To determine if SGs form in these MG, we treated each with sodium arsenite (SA), the most commonly used inducer of SGs. Numerous SGs were found in both cell lines when treated with low concentrations of SA (1 μM) for 24 h as revealed by the appearance of puncta that stained with the SG marker G3BP1 (Fig. 1B). To determine if SYK localized to these SGs, we fixed and stained cells with an antibody against the kinase. A fraction of SYK co-localized with G3BP1 in SGs in both cell types when treated with SA (Fig. 1B). The concentration of SA that was required to induce SGs was surprisingly low compared to the level commonly used to induce SGs in other cell types (McEwen et al., 2005). We then asked if exposure to a stressor known to be involved in neurodegeneration would lead to SG formation. When treated with 100 nM soluble Aβ(1–42) for 24 h, abundant SYK-positive SGs appeared in both BV-2 and N9 cells (Fig. 1C). Quantitative analyses revealed a five-fold increase in area containing co-localized SYK and G3BP1 following treatment with SA or Aβ (Fig. 1D). Cells did not form SGs when treated with Aβ(42–1) (Fig. 1E).

We then asked if other proteins commonly found in SGs were present within these complexes in MG. N9 cells were treated with SA or Aβ for 24 h, fixed and stained for SYK and co-stained for phosphorylated EIF2α, PABP1, TDP-43 and TIA-1. SYK-positive puncta produced by both stimuli contained each of these proteins (Fig. 2A). Similar results were seen in BV-2 cells (Supplemental Fig. 1A). G3BP1 also co-localized in puncta with pEIF2α, TDP-43 and TIA-1 in N9 cells treated with SA or Aβ (Fig. 2B). Since SGs are insoluble in mild detergents, we fractionated control and stressed MG into detergent-soluble and

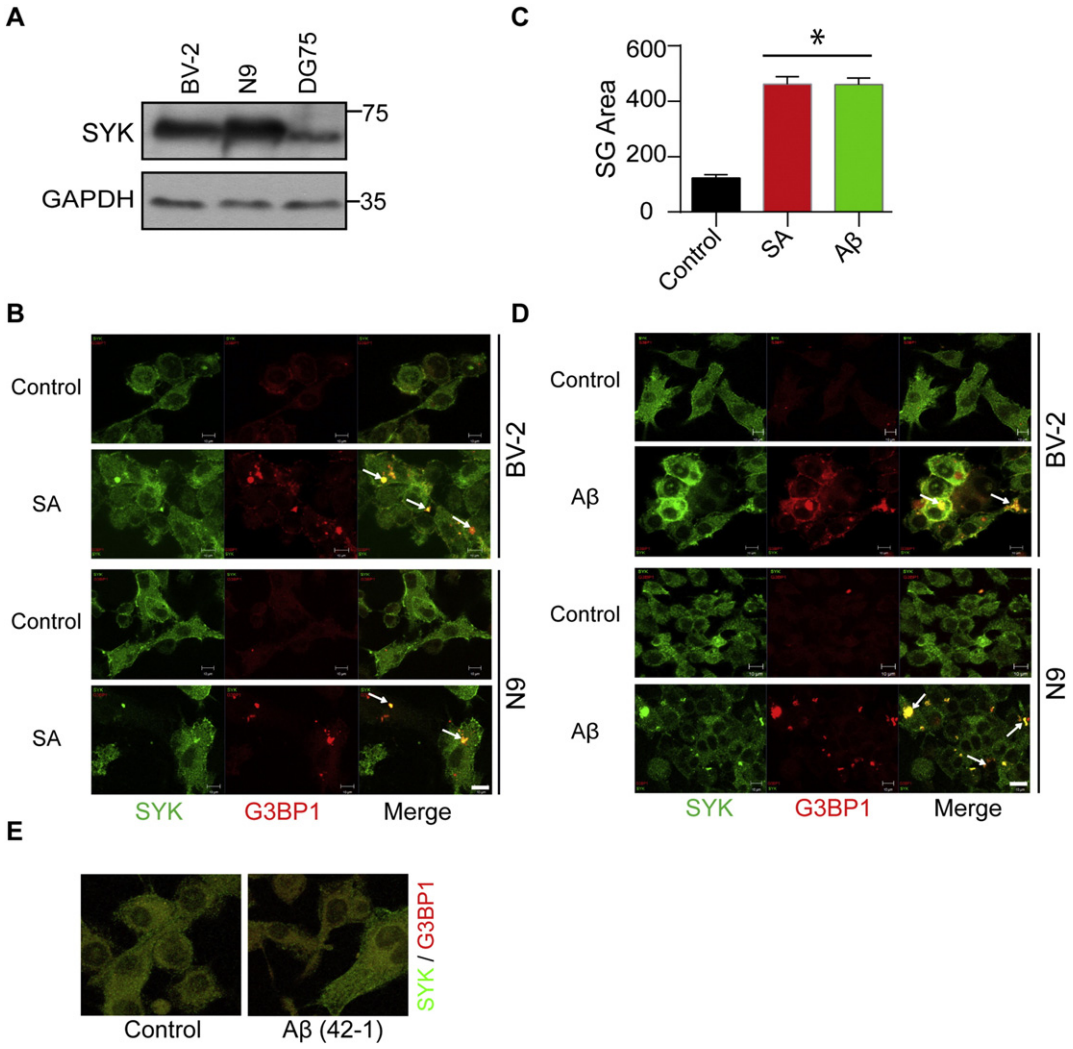

Fig. 1. SYK associates with SGs in MG. (A) Lysates of BV-2, N9 and DG75 cells were examined by Western blotting using antibodies against SYK and GAPDH. (B) BV-2 and N9 cells were treated without (control) or with SA (A) for 24 h, fixed and stained for SYK (green) and G3BP1 (red). Examples of SGs are indicated by the arrows. Bar = 10 μm. (C) The area occupied by SYK and G3BP1 positive SGs in N9 cells was quantified by Image J analysis of 5 random frames from 3 independent experiments. Results represent means ± SEM. *$P = 0.001$. (D) BV-2 and N9 cells were treated without (control) or with soluble Aβ for 24 h, fixed and stained for SYK (green) and G3BP1 (red). Examples of SGs are indicated by the arrows. Bar = 10 μm. (E) BV-2 cells were treated with soluble Aβ(42–1) for 24 h, fixed and stained for SYK (green) and G3BP1 (red). Only merged images are shown.

insoluble fractions and immunoblotted each for SYK, G3BP1, pEIF2α and TIA-1. A significant increase in the presence of SYK, G3BP1, pEIF2α and TIA-1 in the detergent-insoluble fractions accompanied treatment of both N9 cells with either SA or Aβ (Fig. 2C). Similar results were seen with BV-2 cells (Supplemental Fig. 1B). To further confirm an interaction of SYK with SG markers, we expressed SYK-EGFP in BV-2 cells, which were then treated with SA or Aβ, and immunoprecipitated the tagged protein from the SG enriched fraction. Both stress stimuli resulted in an increased association of SYK-EGFP with endogenous SYK, G3BP1 and pEIF2α (Supplemental Fig. 1C).

3.2. SYK is Recruited to SGs in Primary MG

To confirm that SYK also was recruited to SGs in primary cells, we isolated MG from brains of mice either 1 month or 20 months of age. Isolated cells were positive for the MG marker IBA-1, but lacked the astrocyte marker GFAP (Supplemental Fig. 2B & C). When primary MG were treated with SA or Aβ for 24 h, fixed and stained for IBA-1, SYK and G3BP1, we found SYK- and G3BP1-positive puncta formed in response to both stress stimuli. Interestingly, SGs were especially abundant in cells isolated from aged (20 months) animals (Fig. 3A and Supplementary Fig. 2D), indicating that cells from older animals are particularly sensitive to external stress stimuli.

To determine if SYK itself might play a role in the stress-induced formation of SGs, we further compared MG from wild type mice to cells isolated from SYK haploinsufficient mice. MG isolated from the brains of haploinsufficient mice expressed half as much SYK as did cells from wild-type animals (Supplemental Fig. 2B). SG formation was comparable in cells from one month old $Syk^{+/+}$ and $Syk^{+/-}$ animals (Supplemental Fig. 2D & E), but was reduced considerably in cells isolated from the brains of 20 month old $Syk^{+/-}$ mice (Fig. 3B) as compared to their wild-type counterparts (Fig. 3A & C). Since a complete SYK knockout was lethal as seen previously (Turner et al., 1995), we were unable to test cells from $Syk^{-/-}$ animals. These results suggested that SYK may actually promote the formation of SGs in MG.

3.3. SYK Promotes SG Formation

The reduced appearance of SGs in cells from aged mice with reduced levels of SYK as compared to aged mice with normal levels of the kinase suggested a possible role for the kinase in SG induction. To determine if SYK was active when recruited to SGs, we stained control and SA- and

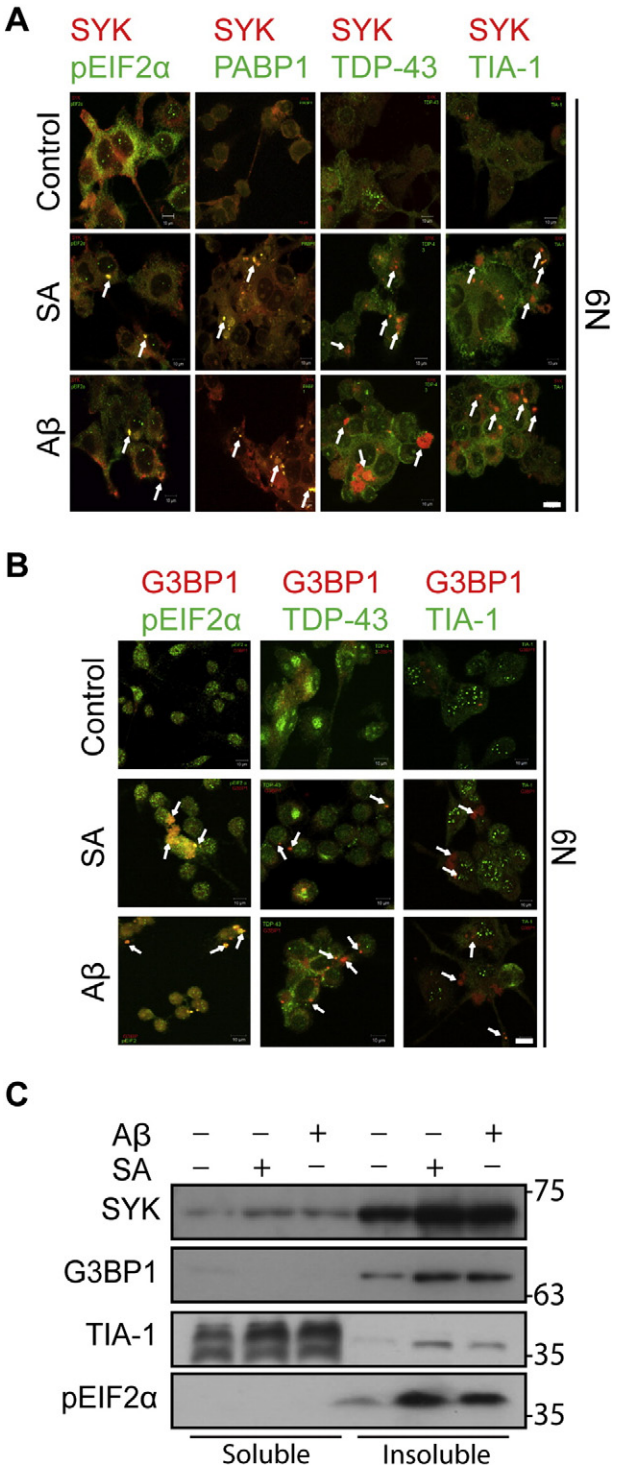

Fig. 2. Characterization of SGs in MG. (A and B) N9 cells were treated without (control) or with SA or soluble Aβ for 24 h, fixed and stained for SYK, pEIF2α, PABP1, TDP-43, TIA-1 and/or G3BP1 as indicated. Only merged images are displayed. Examples of SGs are indicated by the arrows. Bar = 10 μm. (C) N9 cells were treated without (−) or with (+) SA or soluble Aβ for 24 h and then separated into detergent soluble and insoluble fractions, which were analyzed by Western blotting for SYK, G3BP1, TIA-1 and pEIF2α. Data shown are representative of three separate experiments.

Aβ-treated N9 cells with antibodies against SYK and phosphotyrosine. SYK-positive puncta induced by either stimulus contained abundant phosphotyrosine indicating that SYK was active in SGs (Fig. 4A). Similar results were observed in BV-2 cells (Supplemental Fig. 3A). Quantification of images confirmed a significant increase in area containing co-localized SYK and phosphotyrosine (Supplemental Fig. 3B). To confirm the presence of active SYK in SGs, we immunoprecipitated tyrosine-phosphorylated proteins from control, SA- and Aβ-treated N9 cells and immunoblotted the immune complexes for phosphotyrosine and SYK. Induction of SGs with either stimulus resulted in a significant increase in the phosphorylation of multiple proteins including SYK itself (Fig. 4B). Western blotting of lysates of control and SA- or Aβ-treated N9 cells with antibodies specific for the phosphorylated activation loop of SYK confirmed that SYK was active and phosphorylated in response to both stimuli (Fig. 4C).

To determine if active SYK plays a role in SG formation, we stimulated BV-2 cells with SA or Aβ for 24 h in the absence or presence of a SYK inhibitor. We used two distinct inhibitors, R406 and PRT318, to avoid potential complications of off-target effects. In the presence of either inhibitor, neither SA nor Aβ induced the formation of significant SGs (Fig. 4D & E). The ability of each inhibitor to reduce SYK activity was confirmed by the Western blotting with anti-SYK and antiphosphotyrosine antibodies of lysates of BV-2 cells treated with H_2O_2 in the presence or absence of R406 or PRT318. H_2O_2, an inhibitor of tyrosine phosphatases, led to the activation of SYK and its autophosphorylation on Y317 with a resulting shift in its electrophoretic mobility (Keshvara et al., 1998), which was lost in inhibitor-treated cells (Supplemental Fig. 3C).

To further confirm a direct role for SYK in SG formation, we infected BV-2 cells with lentiviruses expressing EGFP and either shRNA against SYK or a scrambled shRNA. SYK levels were selectively reduced in cells expressing the SYK shRNA while levels of G3BP1 were unaffected (Fig. 5A). Infected cells were treated with SA or Aβ for 24 h, fixed and stained for G3BP1. While cells infected with scrambled shRNA readily formed SGs, cells with reduced levels of SYK failed to do so (Fig. 5B and D). As expected, the appearance of SYK in SGs was reduced in the knockdown cells (Fig. 5C).

3.4. Chronic Stress Induces Large and Persistent SGs

SGs formed in cells exposed to SA or Aβ for 24 h were largely cleared within 24 h after removal of the stress stimulus (Supplemental Fig. 4A). However, it has been proposed that exposure to chronic stress leads to the formation of persistent SGs in the brain (Ash et al., 2014). To model this in MG in vitro, we exposed N9 cells to low levels of SA or Aβ for a period of five days to mimic chronic stress. Prolonged stress led to the formation of very large SGs that contained both SYK and G3BP1 (Fig. 6A). To examine the clearance of these SGs, we removed the stress and allowed cells to recover for 48 h. While the intensity of staining for G3BP1 declined somewhat, the area within the cell occupied by SGs was largely unchanged (Fig. 6A and Supplemental Fig. 4B).

3.5. Chronic Stress Induction Leads to SYK-dependent Generation of ROS and RNS

We next explored the possible consequences of the presence of activated SYK in SGs in chronically stressed MG. The receptor-mediated activation of SYK in macrophages and microglial cells is coupled to the production of both ROS and RNS (McDonald et al., 1997; Yi et al., 2014) and the generation of both reactive oxygen and nitrogen species (ROS and RNS) by MG can be damaging to neighboring neuronal cells (Cameron and Landreth, 2010). To determine if chronic stress led to constitutive ROS generation, we treated N9 cells with SA or Aβ for 5 days and then measured the relative amounts of ROS produced over the course of 1 h by monitoring the oxidation of cell permeant DCFDA. Cells chronically stressed by exposure to either SA or Aβ produced substantially more ROS than control cells (Fig. 6B). Similar results were seen when we monitored the conversion of dihydrorhodamine 123 to rhodamine 123 as a measure of ROS production (Fig. 6E). Consistent with these results, cells chronically exposed to either SA or Aβ released substantially more ROS into the media than did untreated cells (Fig. 6C). ROS production in cells treated with either stress stimulus was largely

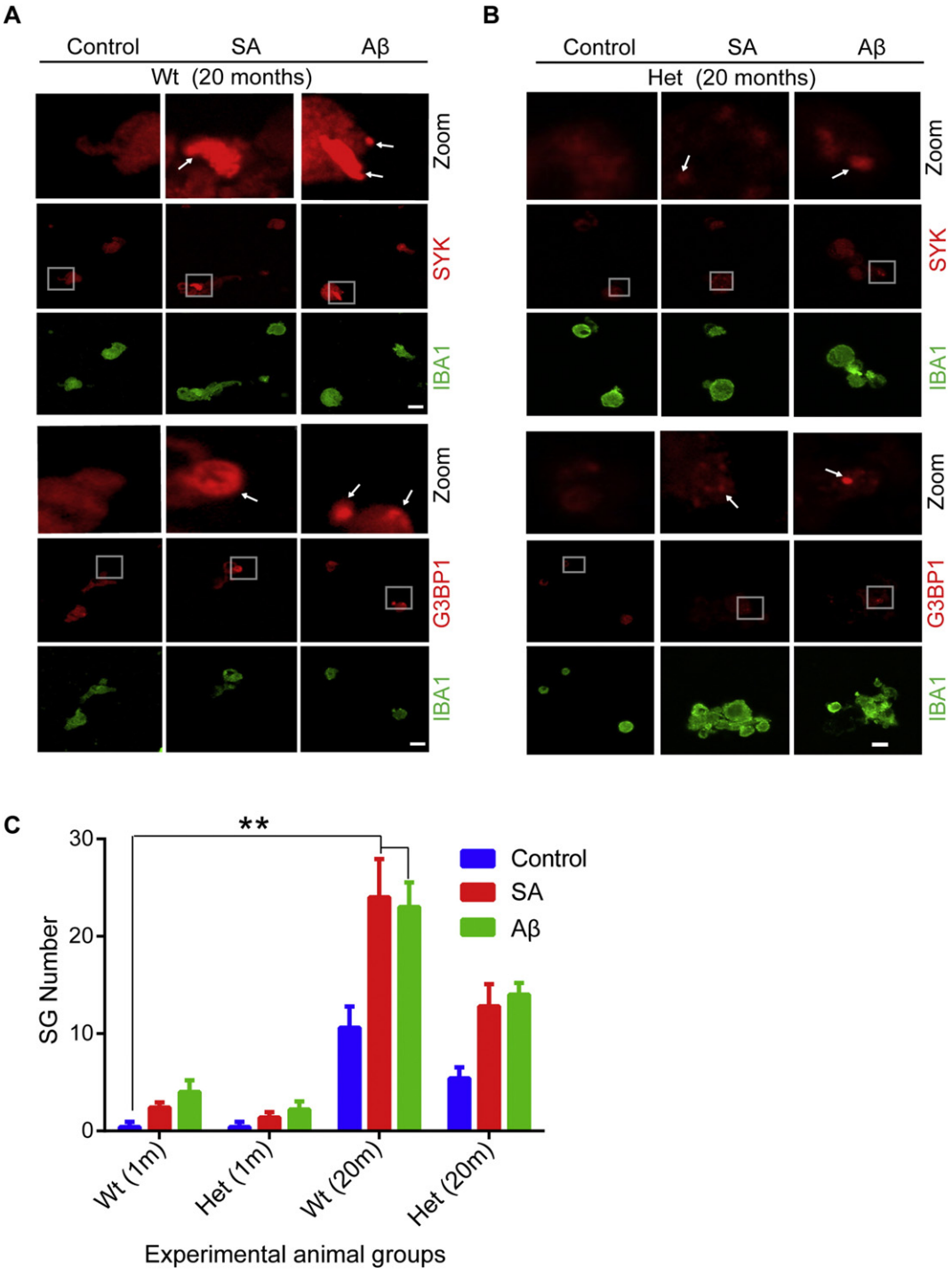

Fig. 3. SYK associates with SGs in MG from aged mice. (A and B) MG isolated from the brains of 20 month old wild-type (A) or *Syk*$^{+/-}$ (B) mice were treated without (control) or with SA or soluble Aβ for 24 h, fixed and co-stained for IBA1 and SYK or IBA1 and G3BP1. Examples of SGs are indicated by the arrows. Bar = 5 μm. (C) Quantitative comparison of SG formation in MG from young (1 m) and old (20 m), wild-type (Wt) and *Syk* haploinsufficient (Het) mice. $^{**}P = 0.001$.

attenuated in the presence of the SYK inhibitor R406 or PRT318 (Fig. 6B, C & E).

Next we examined changes in the release of RNS by measuring nitrite levels in the media. Nitrite release increased three-fold from N9 cells that were chronically stimulated by SA or Aβ (Fig. 6D). Again, levels were reduced significantly if cells were activated in the presence of a SYK inhibitor. Since the formation of RNS in MG is mediated by NOS2 (Mosher and Wyss-Coray, 2014), we measured NOS2 levels in control, SA- and Aβ-treated N9 cells by Western blot (Fig. 6G) and immunofluorescence (Supplemental Fig. 4E). An increase in the expression of NOS2 was observed following both stress stimuli. The induction of NOS2 was reduced substantially in cells in which the activity of SYK was inhibited.

Since ROS and RNS increased in chronically stressed MG, we asked if this could contribute to neuronal cell death. To test this, we co-cultured HT22 neuronal cells with N9 cells separated by a transwell insert. When chronically SA- and Aβ-treated N9 cells were cultured with healthy HT22 cells for two days, we observed a significant increase in annexin

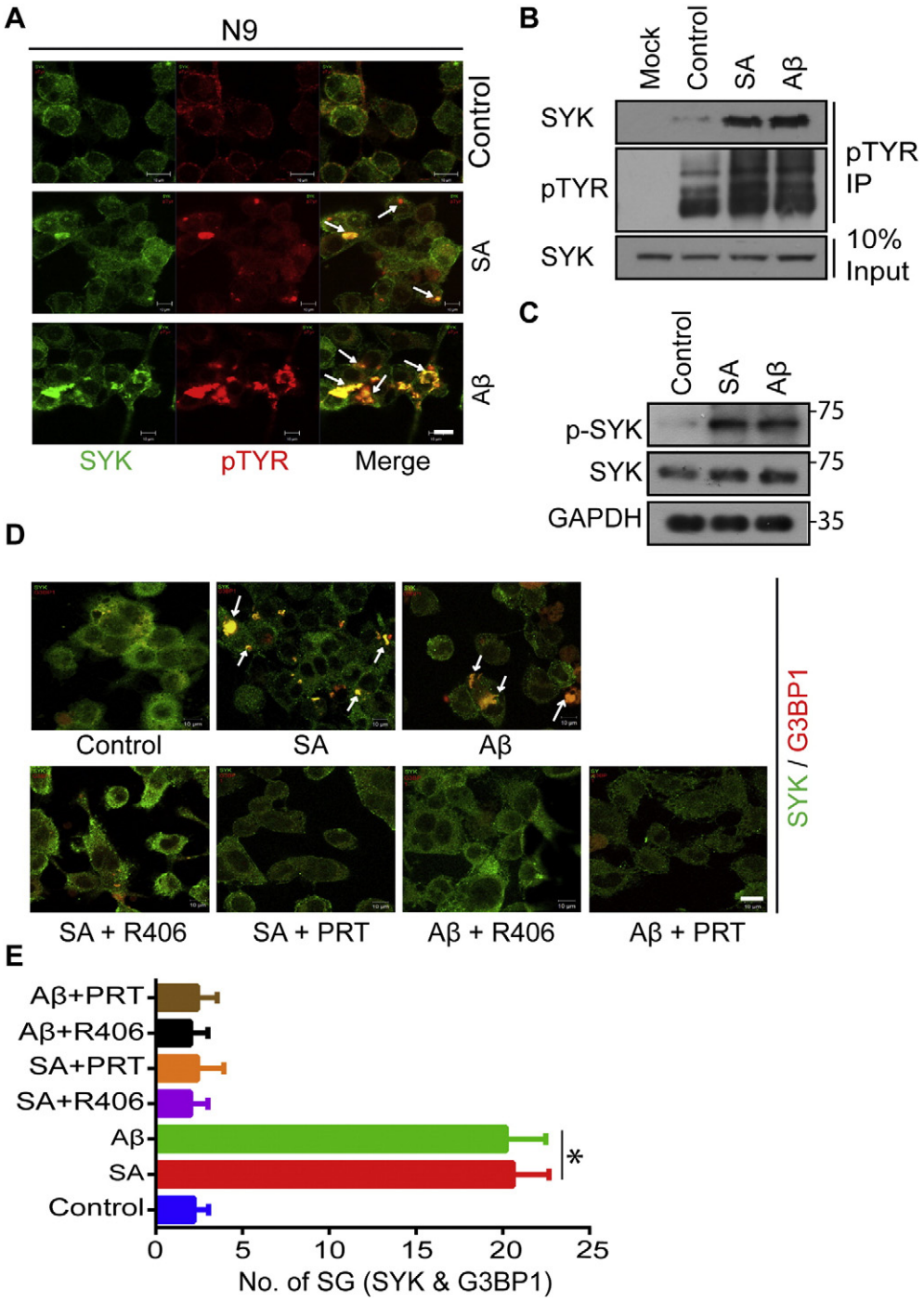

Fig. 4. SYK is active in SGs and promotes their formation. (A) N9 cells were treated without (control) or with SA or soluble Aβ for 24 h, fixed and stained for SYK (green) and phosphotyrosine (pTYR, red). Examples of SGs are indicated by the arrows. Bar = 10 μm. (B) Phosphotyrosine-containing proteins were immunoprecipitated from lysates of N9 cells treated without (control) or with SA or soluble Aβ for 24 h. Immune complexes were examined by Western blotting with antibodies against SYK or phosphotyrosine (pTYR). SYK in the original lysates was detected by Western blotting (input). Beads lacking anti-phosphotyrosine were used as a control (mock). (C) Lysates from N9 cells treated without (control) or with SA or soluble Aβ for 24 h were analyzed by Western blotting using antibodies against SYK phosphorylated on Y519 and Y520 (p-SYK), SYK or GAPDH. (D) N9 cells were treated without (control) or with SA or soluble Aβ for 24 h in the presence or absence of R406 or PRT318 (PRT) (500 nM each), fixed and stained for SYK (green) and G3BP1 (red). Examples of SGs are indicated by the arrows. Bar = 10 μm. (E) The number of SGs formed per cell from (D). Results represent means ± SEM from 3 independent experiments. *$P = 0.0001$.

V binding to HT22 cells (Fig. 6F). Negligible annexin V staining was observed when HT22 cells were cultured with N9 cells that were pretreated with SA or Aβ in the presence of PRT318. To confirm an increase in ROS and RNS in the co-culture media containing activated N9 cells, we measured the levels of each generated over the two day incubation period. A substantial increase in both ROS and RNS was observed when SA- or Aβ-treated N9 cells were co-cultured with HT22 cells (Supplemental Fig. 4C & D). The inhibition of SYK with either PRT318 or R406 reduced the external ROS and RNS levels significantly.

We also compared the media of cells chronically stressed by exposure to Aβ for 120 h in the presence of absence of PRT318 for the secretion of IFNγ, IGF-1, IL-1β, IL-6, leptin, MCP-1, TFGβ and TNFα, relative to levels secreted by untreated cells. The levels of IFN-γ, MCP-1 and IL-1β were significantly increased in chronically stressed cells. Of these, both

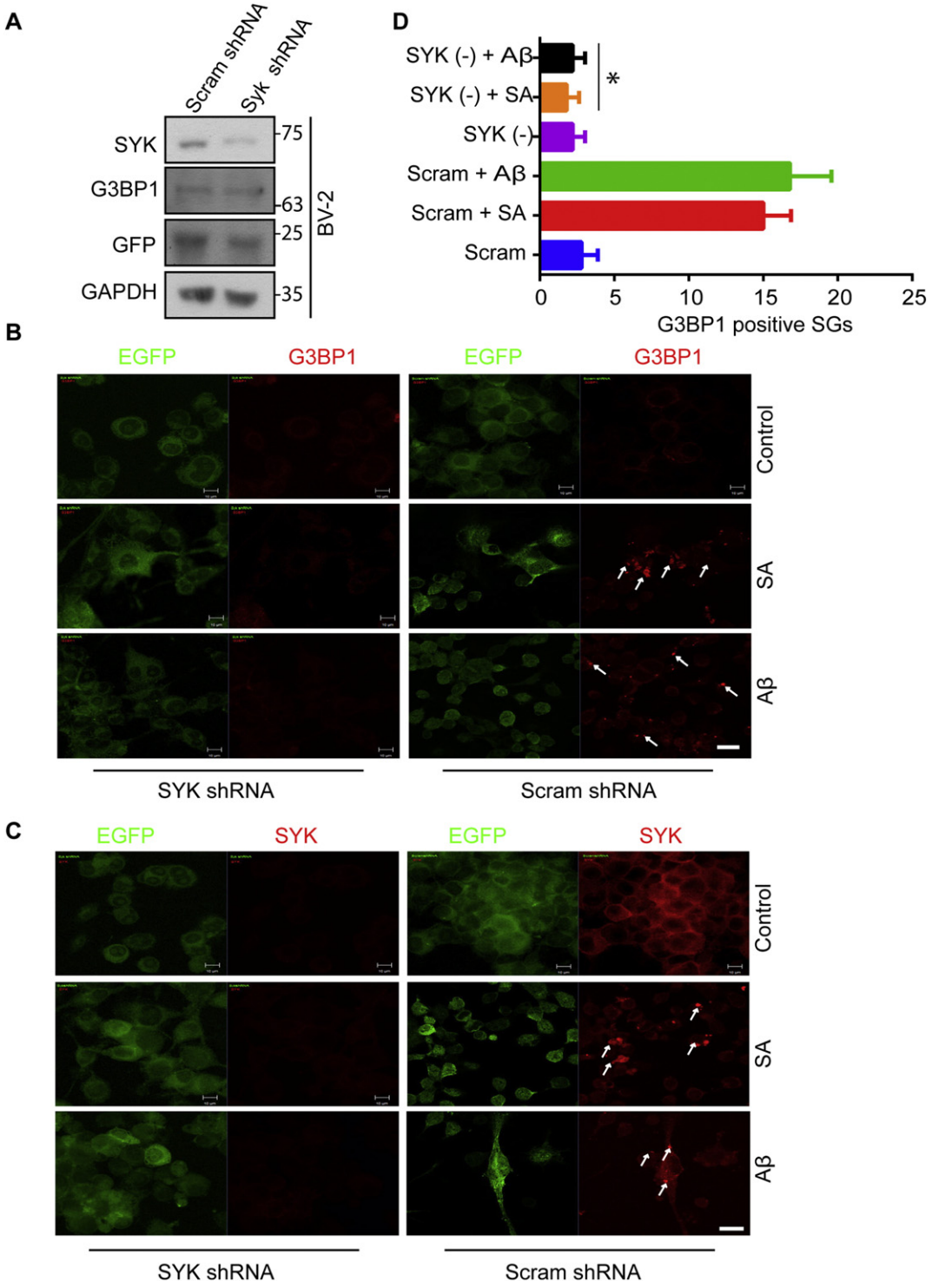

Fig. 5. Reduced SYK inhibits SG formation in MG. (A) BV-2 cells expressing EGFP and scrambled shRNA or SYK shRNA were examined by Western blotting with antibodies against SYK, G3BP1, GFP and GAPDH. (B and C) BV-2 cells infected with a lentivirus expressing EGFP and either a SYK or scrambled shRNA were treated without (control) or with SA or soluble Aβ for 24 h, fixed and stained for G3BP1 (B) or SYK (C) (both in red). Examples of SGs are indicated by the arrows. Bar = 10 μm. (D) Quantification of G3BP1 positive SGs present within 10 random 25× frames for cells expressing SYK shRNA (SYK (−)) or scrambled shRNA (Scram). $^{*}P = 0.001$.

IFN-γ MCP-1 were significantly reduced in the presence of the SYK inhibitor PRT318 (Supplemental Fig. 5A).

3.6. SG Formation in Microglial Cells Impairs Phagocytosis

Despite their apparent activated phenotype, one important function of MG that is compromised in aged and AD brains is phagocytosis. Phagocytosis in myeloid cells through many receptors is a SYK-dependent process, suggesting that the sequestration of SYK in SGs away from membrane-associated phagocytic receptors might compromise their function. To determine if chronic stress negatively affects phagocytic activity, we treated BV-2 or N9 cells with SA or Aβ for 5 days and then assayed the cells for the uptake of pH sensitive *E. coli* BioParticles, which fluoresce only following ingestion. Cells

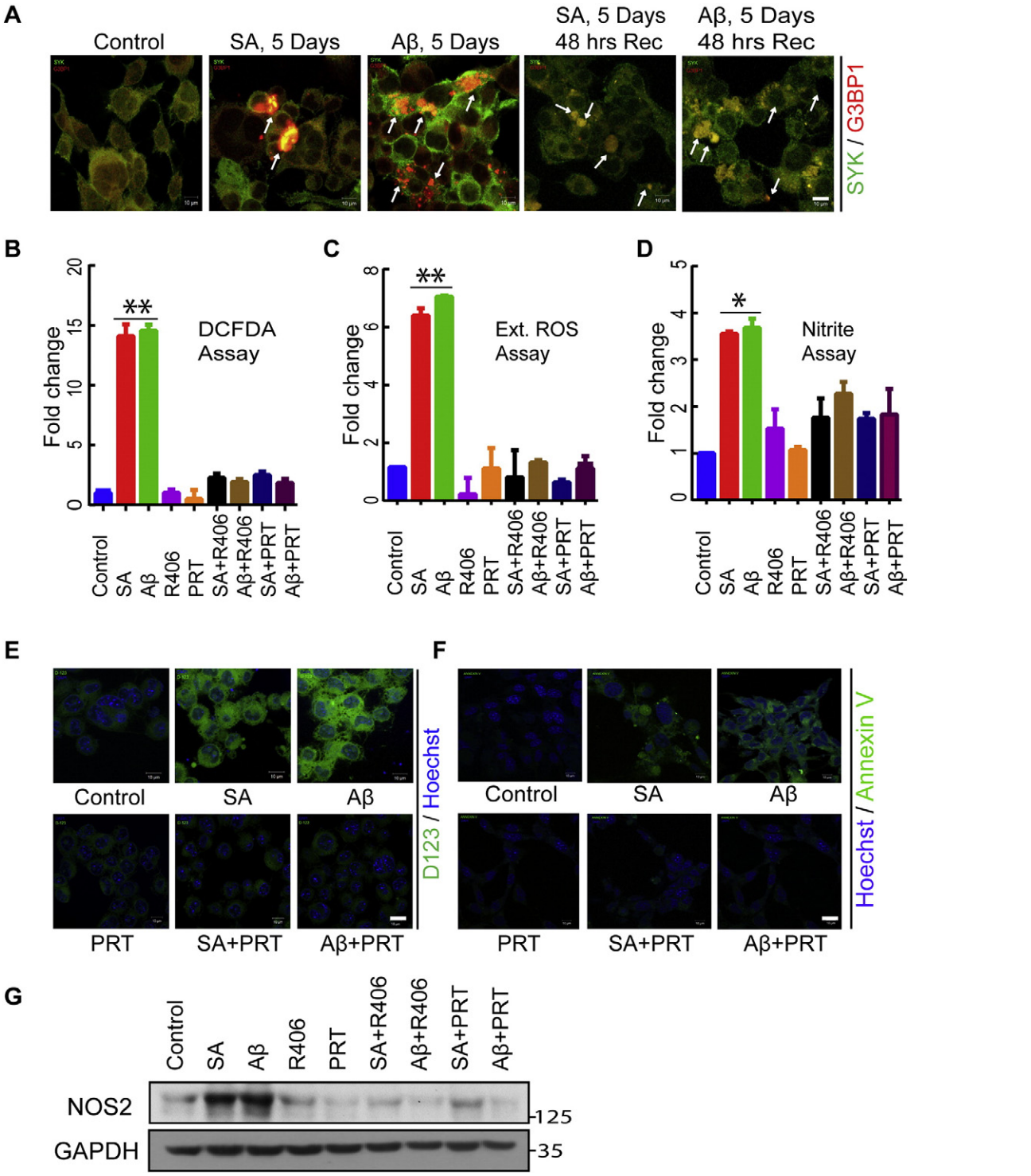

Fig. 6. Chronic stress leads to large SGs and persistent ROS and RNS production. (A) N9 cells were treated without (control) or with SA or soluble Aβ for 5 days. Where indicated, cells were cultured in the absence of SA or Aβ for an additional 48 h. Cells were fixed and stained for SYK (green) and G3BP1 (red). Examples of SGs are indicated by the arrows. Bar = 10 μm. (B-D) N9 cells were treated without (Control) or with SA or Aβ for 5 days in the presence or absence of R406 or PRT318 (500 nM each). Cells were incubated with carboxy-DCFDA (10 μM) for 1 h and examined using a fluorescence plate reader (B). Media was collected and analyzed for ROS using a chemiluminescence assay (C) or nitrite levels using a fluorescence assay (D). Data represent means ± SEM for 3 independent experiments. $^{*}P = 0.001$, $^{**}P = 0.0001$. (E) N9 cells treated without (control) or with SA or Aβ for 5 days in the presence or absence of PRT318 (500 nM) were incubated with D123 for 1 h and green fluorescence was observed by confocal microscopy. Hoechst dye (blue) was used to stain the nucleus. Bar = 10 μm. (F) N9 cells treated for 5 days with SA or Aβ were washed thoroughly and then co-cultured with HT22 for another 48 h separated by a transwell insert. HT22 cells were incubated with FITC Annexin V (green) for 30 min, fixed and imaged by confocal microscopy. Hoechst dye (blue) was used to stain the nucleus. Bar = 10 μm. (G) Lysates from the cells in (D) were analyzed by Western blotting for NOS2 and GAPDH.

were either fixed and stained as shown in Fig. 7A for BV-2 cells or examined by live cell imaging as shown for N9 cells in Supplemental Movies 1–3. For both cell types, chronic stress induced by either SA or Aβ strongly impaired the uptake of the pHRhodo particles. Phagocytic activity was inhibited as well when cells were treated with either R406 or PRT318 even in the absence of SA or Aβ supporting an important role for SYK in phagocytosis (Fig. 7A & B). Uptake of pHRhodo particles was blocked by the incubation of cells

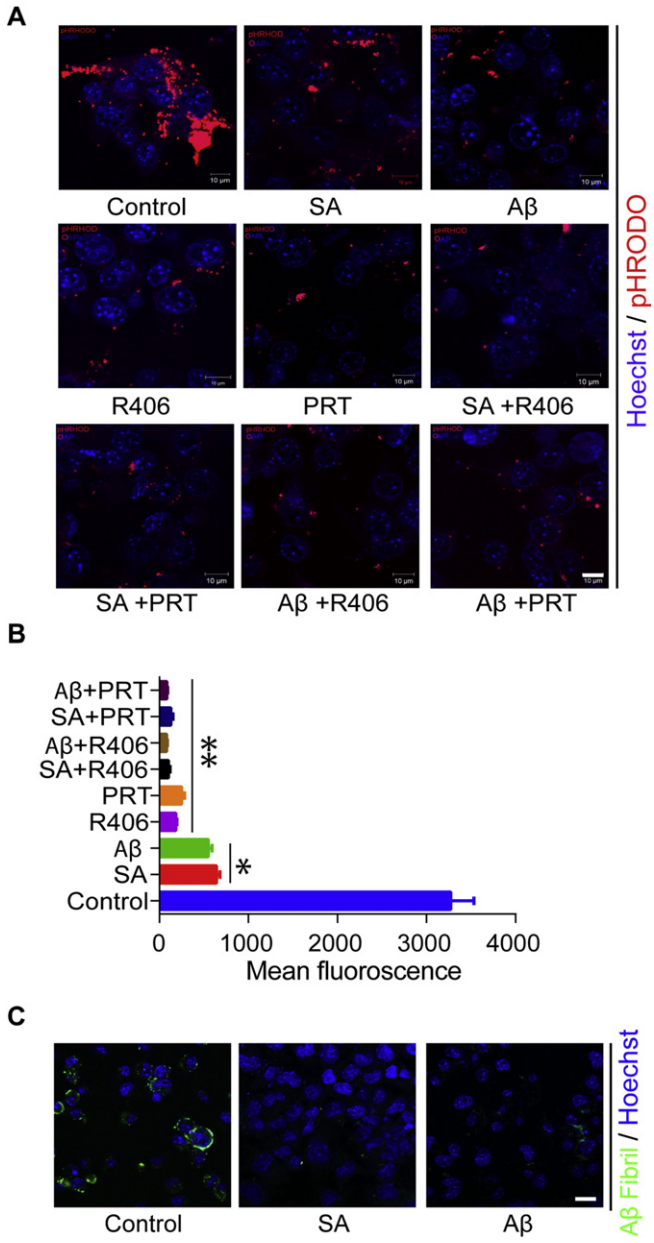

Fig. 7. SYK inhibitors or chronic stress block MG phagocytosis. (A) BV-2 cells were treated without (control) or with SA or soluble Aβ for 5 days in the presence or absence of R406 or PRT381 (500 nM each) and examined for the uptake of pHRodo particles (red). Cells were fixed and examined by confocal microscopy. Hoechst dye (blue) was used to stain the nucleus. Bar = 10 μm. (B) Quantification of (A) showing change in mean fluorescence measured by Image J from ten random frames in three independent experiments. $^{*}P = 0.001$ as compared to control cells, $^{**}P = 0.0001$ as compared to control cells. (C) N9 cells treated without (control) or with SA or soluble Aβ for 5 days were incubated with FITC-labeled Aβ fibrils for 12 h, washed, fixed and examined by confocal microscopy. Hoechst dye (blue) was used to stain the nucleus.

with cytochalasin D, consistent with phagocytosis as a mechanism of particle uptake (Supplemental Fig. 5B).

An important function of MG is to clear β-amyloid plaques. To examine the effects of stress on this process, we treated N9 cells with SA or Aβ for 5 days and measured their ability to take up fluorescein-labeled Aβ fibrils. Again, control cells readily phagocytosed Aβ fibrils whereas chronically stressed cells were unable to do so (Fig. 7C & Supplemental Fig. 5D). Similar to soluble Aβ, Aβ fibrils also induced the formation of SGs containing both SYK and G3BP1 when added to either BV-2 or N9 cells (Supplemental Fig. 5E).

3.7. SYK Associated SGs are Formed in Brains of AD Patients

MG in patients with AD are chronically exposed to external sources of stress including interactions with Aβ aggregates. Since prolonged stress of MG in vitro resulted in the development of persistent SGs to which SYK was recruited, we asked if a similar response might be associated with AD. To explore this, we examined brain samples from patients with no, mild, moderate or severe AD (Supplemental Table 1). Paraffin-fixed sections of brain cortex were stained with antibodies against IBA1, SYK, G3BP1 and/or phosphotyrosine. SYK was diffusely distributed in MG in patients with no AD and in patients with mild disease, but was increasingly present in large puncta with escalating disease severity (Fig. 8A & Supplemental Table 1). SYK co-localized within these puncta in diseased brain with both G3BP1 and phosphotyrosine indicating that the kinase was localized to SGs and was active at these sites (Fig. 8B & C).

3.8. Recovery of Impaired Phagocytosis by IgG

We then asked if manipulations of SYK activity or localization might restore the ability of chronically stressed MG to phagocytose foreign particles. Since integrin ligation leads to the activation of SYK in macrophages (Mócsai et al., 2006), we first treated chronically stressed N9 cells with rabbit IgG directed against β1 integrin. Treatment of stressed N9 cells for 4 h led to a marked recovery of phagocytic activity (Fig. 9A). As a control, we treated stressed N9 cells with nonspecific rabbit IgG isotype control antibodies. Interestingly, phagocytic activity was again restored (Fig. 9A). To explore this further, we treated stressed cells with an affinity purified rabbit IgG directed against a peptide from the cytoplasmic C-terminus of the inhibitory receptor CD32, an antibody that should neither react with intact MG nor activate SYK. Again, incubation with this antibody led to a recovery of phagocytic activity in chronically stressed cells (Fig. 9A). Thus, phagocytic activity in stressed MG could be restored by treatment with IgG independent of the specificity of the antibody.

To explore a mechanism for the recovery of phagocytic activity, we examined the effects of IgG on the localization of SYK in the cell. Treatment of N9 cells with either non-specific rabbit IgG or the anti-CD32 antibody led to a relocalization of SYK from the cytoplasm to the plasma membrane, the site where phagocytosis takes place. Even in chronically stressed cells, a substantial amount of SYK was translocated from SGs to the membrane (Fig. 9B). Western blotting of detergent-soluble fractions of N9 cells confirmed the partial re-location of SYK to the detergent-soluble fraction following incubation with rabbit IgG or anti-CD32 (Supplemental Fig. 6). These results indicate that it may be possible to restore the phagocytic activity of chronically stressed MG by manipulating the intracellular localization of SYK.

4. Discussion

Paradoxically, MG from aged and AD brain exhibit a phenotype that combines a perpetually activated state with functionally impaired phagocytic activity (Gandy and Heppner, 2013; Mosher and Wyss-Coray, 2014). To explain this dichotomy, we propose a model in which the altered activity and localization of SYK contributes to both phenotypes. In this model, chronic stress leads to the formation of SGs to which SYK is recruited resulting both in a pro-inflammatory phenotype and impaired phagocytosis. Impaired phagocytosis leads to further accumulation of Aβ plaques that potentiate SG formation leading to persistent inflammation and neuronal cell damage.

SG formation is thought to be, at least initially, a defense against stress, providing a mechanism for the selective sequestration and protection from degradation of a subset of mRNAs (Anderson and Kedersha, 2008). However, it is clear that persistent formation of RNP particles is deleterious to cells as noted for several neurodegenerative disorders where aggregates appear in neuronal cells (Harris and

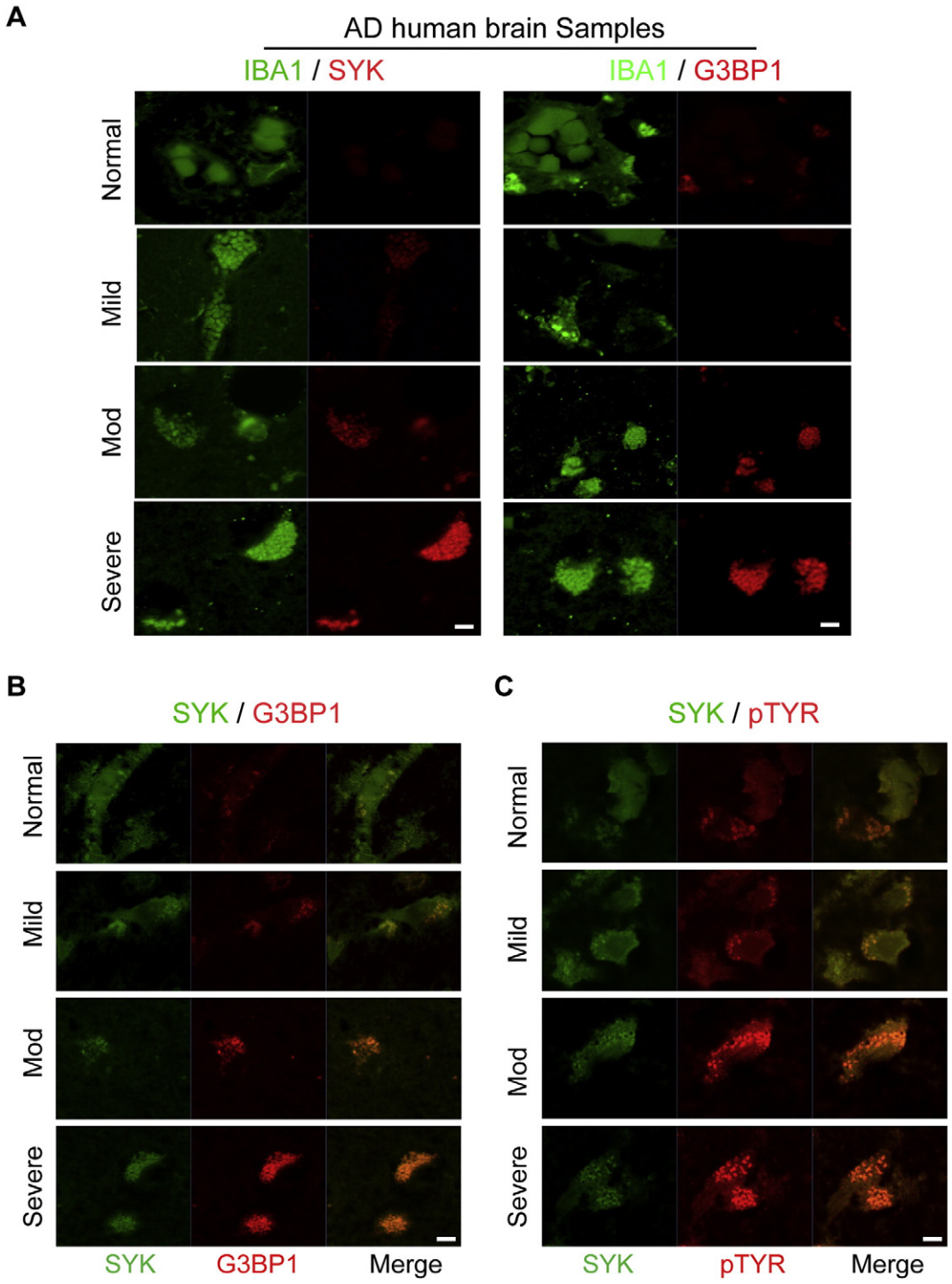

Fig. 8. SYK, G3BP1 and phosphotyrosine-positive SGs are found in AD brains. (A–C) Samples from the cortex region of human brain from patients with no (normal), mild, moderate (mod) and severe AD were immunostained for IBA1, SYK, G3BP1 and/or phosphotyrosine (pTYR) as indicated. Bar = 5 μm.

Rubinsztein, 2011; Menzies et al., 2015). Our data indicate that SGs form, as well, in MG. In fact, MG appear particularly susceptible to the stress-induced formation of SGs as their induction requires exposure only to low levels of SA or Aβ.

The recruitment of SYK to SGs in non-inflammatory cells protects them from short-term, stress-induced damage by stimulating SG clearance through autophagy, an event that requires both SYK activity and its association with SGs (Krisenko et al., 2015). This process may be operative as well in MG as SGs can be cleared effectively from cells exposed to stress for short periods of time. However, prolonged stress leads to the formation of large SGs that associate with SYK and are resistant to clearance as they persist following removal of the stimulus. We find that large SGs are characteristic of MG in the brains of patients with advanced AD, suggesting that these cells have been exposed to persistent stress stimuli. This is consistent with observations that oxidative stress often precedes the pathogenesis of AD since enhanced neuroinflammation resulting from traumatic brain injury or infection predispose individuals to AD (Perry et al., 2002; Griffin, 2013) while the long-term use of NSAIDS can be protective (Vlad et al., 2008). The pronounced sensitivity of primary MG from aged mice to SA- or Aβ-induced SGs suggests that MG in the brains of elderly patients may be particularly prone to the stress-induced formation of SGs consistent with advanced age as the

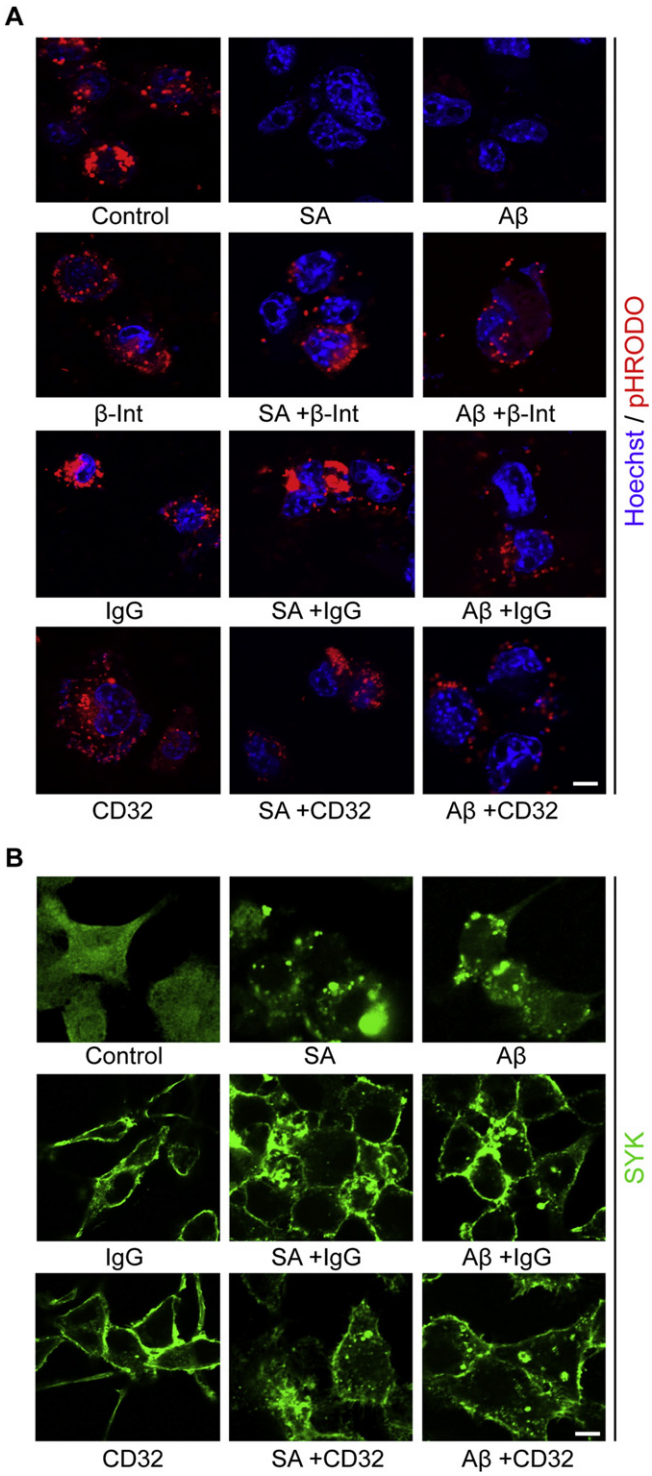

Fig. 9. Restoration of phagocytic activity with IgG. (A and B) N9 cells were treated without (control) or with SA or soluble Aβ for 120 h in the presence or absence of R406 or PRT318 (500 nM each). At 116 h, to one set of control, SA- and Aβ-treated cells was added anti-β1-integrin (β-Int), mixed rabbit IgG (IgG) or anti-CD32 for the final 4 h. Cells were then incubated with pHRhodo particles (red) to measure phagocytosis (A) or fixed and stained with antibodies against SYK (B). Hoechst dye (blue) was used to stain the nucleus (A). Bar = 10 μm.

leading risk factor for AD (Cameron and Landreth, 2010). The appearance of SYK- and phosphotyrosine-containing puncta in brain samples may serve as a useful marker of stressed and dysfunctional MG in neurodegenerative disease.

The formation of SGs in MG in response to low levels of either SA or Aβ requires the activity and expression of SYK as it is blocked by SYK inhibitors or by a knockdown or reduction of SYK expression. In inflammatory cells like MG, SYK plays a well known role in the receptor-mediated production of ROS and RNS (Yi et al., 2014). Aβ binds to MG via an assortment of cell surface receptors (Mosher and Wyss-Coray, 2014) many of which, including CD14, TLR4, CD36, and SIRPβ1, are coupled to SYK either directly or through receptor-associated proteins that contain ITAMs (Miller et al., 2012; Heit et al., 2013; Gaikwad et al., 2009; Dietrich et al., 2000; Bamberger et al., 2003). The interactions of microglial cells with Aβ leads to the phosphorylation and activation of LYN and SYK, which are coupled to the generation of superoxide radicals and lead to neurotoxicity (McDonald et al., 1997; Combs et al., 1999; Sondag et al., 2009). SYK also is activated in cells under conditions of increased oxidative stress (Schieven et al., 1993). The resulting SYK-dependent pro-inflammatory response may be further exacerbated by the retention within SGs of active SYK—as reflected by the presence of phosphotyrosine-containing proteins—which may continue to stimulate downstream signaling pathways that generate ROS or RNS. The production of ROS and RNS can be damaging to neighboring cells (Mosher and Wyss-Coray, 2014) and we find, in fact, that chronically activated MG produce mediators that are toxic to HT22 neuronal cells. Consistent with a role for SYK in these processes, the generation of chronically activated MG that produce ROS and RNS and the ability of these cells to kill neuronal cells are all blocked by SYK inhibitors. Interestingly, chronically stressed MG also produce increased quantifies of IFNγ and MCP-1/CCL2, cytokines reported previously to be produced by MG in response to stress associated with Parkinson's disease or inflammation (Barcia et al., 2012; D'Mello et al., 2009).

The ability of MG to clear Aβ plaques through phagocytosis is important for the control of AD (Bamberger et al., 2003; El Khoury et al., 2007). Chronic stress induced by prolonged exposure of MG to either SA or Aβ inhibits the ability of these cells to phagocytose either bacteria or Aβ fibrils. Since the chronic stimulation of MG with either SA or Aβ results in the formation of very large SGs to which SYK is recruited, we propose that it is the sequestration of the kinase away from phagocytic receptors that underlies the impaired phagocytic activity of MG. An enhanced accumulation of Aβ plaques in the brain would be an expected result of exposure to oxidative stress due to this loss of phagocytic activity of stressed MG. The exposure of MG to Aβ or Aβ fibrils alone also induces the appearance of abundant SGs, consistent with the known ability of Aβ to trigger MG cell activation and promote the generation of ROS and RNS (Bianca et al., 1999; Combs et al., 2001). Thus, a defect in the removal of Aβ fibrils by MG compromised by oxidative stress could cause a build-up of Aβ plaques leading to additional Aβ-induced stress and the enhanced formation of persistent SGs. In a mouse model of AD, the phagocytic activity of MG is selectively compromised in brain regions containing Aβ plaques (Krabbe et al., 2013). This would be particularly problematic in aged brains as our evidence indicates that MG from older mice are more sensitive to Aβ-induced formation of SGs.

The critical role that SYK plays in modulating immune cell signaling pathways has generated considerable interest in the development of inhibitors of SYK for the treatment of inflammatory diseases (Geahlen, 2014) including, recently, Alzheimer's disease (Paris et al., 2014). While SYK inhibitors might reasonably be expected to reduce the activation of MG and production of inflammatory mediators, inhibitors also block phagocytosis. This may complicate the development of strategies for the use of specific SYK inhibitors for the treatment or prevention of AD. However, the finding that active SYK is sequestered in SGs suggests that strategies to relocate the enzyme might be effective in restoring some function to damaged MG. We find that the treatment of chronically stressed MG with rabbit IgG leads to a dramatic restoration of phagocytic activity. The recovery of activity is not a function of the reactivity of the IgG to any specific antigen as even an affinity-purified antibody prepared against a peptide found on the cytoplasmic domain of an ITIM-containing receptor is able to induce this effect. Treatment

of MG with IgG leads to a relocalization of SYK from the cytoplasm to the plasma membrane in unstressed cells and from SGs to the membrane in chronically stressed cells. This effect may help explain the therapeutic benefits of intravenous immunoglobulins (IVIg), which have shown efficacy in slowing the progression of AD in some human clinical trials (Dodel et al., 2002; Dodel et al., 2004; Relkin et al., 2009; Loeffler, 2013). The benefits of IVIg are generally attributed to the presence of anti-Aβ antibodies in the pooled IgG preparations (Dodel et al., 2004). However, it is interesting to note that the administration of pooled mouse IgG having no detectable anti-Aβ activity to the brains of APP/PS1 mice leads to a reduction in Aβ deposits similar to IVIg (Sudduth et al., 2013). Thus, even immunoglobulins that fail to recognize Aβ have the potential to reverse defects in the function of stressed MG. This observation suggests that the development of IgG-related therapeutics optimized for the recovery of phagocytic activity of MG would be an attractive strategy for augmenting current strategies for the treatment of AD.

Supplementary data to this article can be found online at http://dx.doi.org/10.1016/j.ebiom.2015.09.053.

Author Contributions

S.G. and R.L.G. conceived of the project and contributed to experimental design. S.G. performed all experiments. S.G. and R.L.G. wrote the manuscript.

Conflicts of Interest

None.

Acknowledgments

This work was supported by grant R01 AI098132 (R.L.G.) awarded by the National Institute of Allergy and Infectious Diseases. The transgenic mouse and DNA sequencing facilities were supported by NCI CCSG CA23168 to the Purdue University Center for Cancer Research. The Brain and Body Donation Program was supported by National Institute of Neurological Disorders and Stroke, U24NS072026 National Brain and Tissue Resource for Parkinson's Disease and Related Disorders; National Institute on Aging, P30 AG19610 Arizona Alzheimer's Disease Core Center; Arizona Department of Health Services, Arizona Alzheimer's Consortium; Arizona Biomedical Research Commission, Arizona Parkinson's disease Consortium; and the Michael J. Fox Foundation for Parkinson's Research.

References

Anderson, P., Kedersha, N., 2008. Stress granules: the Tao of RNA triage. Trends Biochem. Sci. 33, 141–150.

Angata, T., Kerr, S.C., Greaves, D.R., Varki, N.M., Crocker, P.R., Varki, A., 2002. Cloning and characterization of human siglec-11: a recently evolved signaling molecule that can interact with SHP-1 and SHP-2 and is expressed by tissue macrophages, including brain microglia. J. Biol. Chem. 277, 24466–24474.

Ash, P.E., Vanderweyde, T.E., Youmans, K.L., Apicco, D.J., Wolozin, B., 2014. Pathological stress granules in Alzheimer's disease. Brain Res. 1584, 52–58.

Bamberger, M.E., Harris, M.E., McDonald, D.R., Husemann, J., Landreth, G.E., 2003. A cell surface receptor complex for fibrillar beta-amyloid mediates microglial activation. J. Neurosci. 23, 2665–2674.

Barcia, C., Ross, C.M., Annese, V., Gómez, A., Ros-Bernal, F., Aguado-Llera, D., Martinez-Pagán, E., de Pablos, V., Fernandez-Villalba, E., Herrero, M.T., 2012. IFN-γ signaling, with the synergistic contribution of TNF-α, mediates cell specific microglial and astroglial activation in experimental models of Parkinson's disease. Cell Death Dis. 3, e379. http://dx.doi.org/10.1038/cddis.2012.123.

Beach, T.G., Adler, C.H., Sue, L.I., Serrano, G., Shill, H.A., Walker, D.G., Lue, L., Roher, A.E., Dugger, B.N., Maarouf, C., Birdsill, A.C., Intorcia, A., Saxon-Labelle, M., Pullen, J., Scroggins, A., Filon, J., Scott, S., Hoffman, B., Garcia, A., Caviness, J.N., Hentz, J.G., Driver-Dunckley, E., Jacobson, S.A., Davis, K.J., Belden, C.M., Long, K.E., Malek-Ahmadi, M., Powell, J.J., Gale, L.D., Nicholson, L.R., Caselli, R.J., Woodruff, B.K., Rapscak, S.Z., Ahern, G.L., Shi, J., Burke, A.D., Reiman, E.M., Sabbagh, M.N., 2015. Arizona study of aging and neurodegenerative disorders and brain and body donation program. Neuropathology. http://dx.doi.org/10.1111/neup.12189.

Bertram, L., Lange, C., Mullin, K., Parkinson, M., Hsiao, M., Hogan, M.F., Schjeide, B.M., Hooli, B., Divito, J., Ionita, I., Jiang, H., Laird, N., Moscarillo, T., Ohlsen, K.L., Elliott, K., Wang, X., Hu-Lince, D., Ryder, M., Murphy, A., Wagner, S.L., Blacker, D., Becker, K.D., Tanzi, R.E., 2008. Genome-wide association analysis reveals putative Alzheimer's disease susceptibility loci in addition to APOE. Am. J. Hum. Genet. 83, 623–632.

Bianca, V.D., Dusi, S., Bianchini, E., Dal Prà, I., Rossi, F., 1999. Beta-amyloid activates the O-2 forming NADPH oxidase in microglia, monocytes, and neutrophils. A possible inflammatory mechanism of neuronal damage in Alzheimer's disease. J. Biol. Chem. 274, 15493–15499.

Blasi, E., Barluzzi, R., Mazzolla, R., Bistoni, F., 1990. Immortalization of murine microglial cells by a v-raf/v-myc carrying retrovirus. J. Neuroimmunol. 27, 229–237.

Buchan, J., Parker, R., 2009. Eukaryotic stress granules: the ins and outs of translation. Mol. Cell 36, 932–941.

Buchan, J.R., Kolaitis, R.-M., Taylor, J.P., Parker, R., 2013. Eukaryotic stress granules are cleared by autophagy and Cdc48/VCP function. Cell 153, 1461–1474.

Cambier, J.C., 1995. New nomenclature for the Reth motif (or ARH1/TAM/ARAM/YXXL). Immunol. Today 16, 110.

Cameron, B., Landreth, G., 2010. Inflammation, microglia, and Alzheimer's disease. Neurobiol. Dis. 37, 503–509.

Combs, C.K., Johnson, D.E., Cannady, S.B., Lehman, T.M., Landreth, G.E., 1999. Identification of microglial signal transduction pathways mediating a neurotoxic response to amyloidogenic fragments of beta-amyloid and prion proteins. J. Neurosci. 19, 928–939.

Combs, C.K., Karlo, J.C., Kao, S.C., Landreth, G.E., 2001. Beta-amyloid stimulation of microglia and monocytes results in TNFalpha-dependent expression of inducible nitric oxide synthase and neuronal apoptosis. J. Neurosci. 21, 1179–1188.

Crowley, M.T., Costello, P.S., Fitzer-Attas, C.J., Turner, M., Meng, F., Lowell, C., Tybulewicz, V.L., DeFranco, A.L., 1997. A critical role for SYK in signal transduction and phagocytosis mediated by fcγ receptors on macrophages. J. Exp. Med. 186, 1027–1039.

Dahlgren, K.N., Manelli, A.M., Stine Jr., W.B., Baker, L.K., Krafft, G.A., LaDu, M.J., 2002. Oligomeric and fibrillar species of amyloid-beta peptides differentially affect neuronal viability. J. Biol. Chem. 277, 32046–32053.

Davis, J.B., Maher, P., 1994. Protein kinase C activation inhibits glutamate-induced cytotoxicity in a neuronal cell line. Brain Res. 652, 169–173.

Dietrich, J., Cella, M., Seiffert, M., Bühring, H.J., Colonna, M., 2000. Signal-regulatory protein beta 1 is a DAP12-associated activating receptor expressed in myeloid cells. J. Immunol. 164, 9–12.

D'Mello, C., Le, T., Swain, M.G., 2009. Cerebral microglia recruit monocytes into the brain in response to tumor necrosis factorα signaling during peripheral organ inflammation. J. Neurosci. 29, 2089–2102.

Dodel, R., Hampel, H., Depboylu, C., Lin, S., Gao, F., Schock, S., Jäckel, S., Wei, X., Buerger, K., Höft, C., Hemmer, B., Möller, H.J., Farlow, M., Oertel, W.H., Sommer, N., Du, Y., 2002. Human antibodies against amyloid beta peptide: a potential treatment for Alzheimer's disease. Ann. Neurol. 52, 253–256.

Dodel, R.C., Du, Y., Depboylu, C., Hampel, H., Frölich, L., Haag, A., Hemmeter, U., Paulsen, S., Teipel, S.J., Brettschneider, S., Spottke, A., Nölker, C., Möller, H.J., Wei, X., Farlow, M., Sommer, N., Oertel, W.H., 2004. Intravenous immunoglobulins containing antibodies against beta-amyloid for the treatment of Alzheimer's disease. J. Neurol. Neurosurg. Psychiatry 75, 1472–1474.

El Khoury, J., Toft, M., Hickman, S.E., Means, T.K., Terada, K., Geula, C., Luster, A.D., 2007. Ccr2 deficiency impairs microglial accumulation and accelerates progression of Alzheimer-like disease. Nat. Med. 13, 432–438.

Gaikwad, S., Larionov, S., Wang, Y., Dannenberg, H., Matozaki, T., Monsonego, A., Thal, D.R., Neumann, H., 2009. Signal regulatory protein-beta1: a microglial modulator of phagocytosis in Alzheimer's disease. Am. J. Pathol. 175, 2528–2539.

Galan, J., Paris, L.L., Zhang, H.-J., Adler, J., Geahlen, R.L., Tao, W.A., 2011. Identification of SYK-interacting proteins using a novel amine-specific isotope tag and GFP nanotrap. J. Am. Soc. Mass Spectrom. 22, 319–328.

Gandy, S., Heppner, F.L., 2013. Microglia as dynamic and essential components of the amyloid hypothesis. Neuron 78, 575–577.

Geahlen, R.L., 2009. SYK and pTyr'd: signaling through the B cell antigen receptor. Biochim. Biophys. Acta 1793, 1115–1127.

Geahlen, R.L., 2014. Getting Syk: spleen tyrosine kinase as a therapeutic target. Trends Pharmacol. Sci. 35, 414–422.

Goggin, K., Beaudoin, S., Grenier, C., Brown, A.A., Roucou, X., 2008. Prion protein aggresomes are poly(A) ribonucleoprotein complexes that induce a PKR-mediated deficient cell stress response. Biochim. Biophys. Acta 1783, 479–491.

Griciuc, A., Serrano-Pozo, A., Parrado, A.R., Lesinski, A.N., Asselin, C.N., Mullin, K., Hooli, B., Choi, S.H., Hyman, B.T., Tanzi, R.E., 2013. Alzheimer's disease risk gene CD33 inhibits microglial uptake of amyloid beta. Neuron 78, 631–643.

Griffin, W.S.T., 2013. Neuroinflammatory cytokine signaling and Alzheimer's disease. N. Engl. J. Med. 368, 770–771.

Guerreiro, R., Wojtas, A., Bras, J., Carrasquillo, M., Rogaeva, E., Majounie, E., Cruchaga, C., Sassi, C., Kauwe, J.S., Younkin, S., Hazrati, L., Collinge, J., Pocock, J., Lashley, T., Williams, J., Lambert, J.C., Amouyel, P., Goate, A., Rademakers, R., Morgan, K., Powell, J., St George-Hyslop, P., Singleton, A., Hardy, J., Alzheimer Genetic Analysis Group, 2013. TREM2 variants in Alzheimer's disease. N. Engl. J. Med. 368, 117–127.

Harris, H., Rubinsztein, D.C., 2011. Control of autophagy as a therapy for neurodegenerative disease. Nat. Rev. Neurol. 8, 108–117.

Heit, B., Kim, H., Cosio, G., Castaño, D., Collins, R., Lowell, C.A., Kain, K.C., Trimble, W.S., Grinstein, S., 2013. Multimolecular signaling complexes enable SYK-mediated signaling of CD36 internalization. Dev. Cell 24, 372–383.

Hickman, S.E., Allison, E.K., El Khoury, J., 2008. Microglial dysfunction and defective beta-amyloid clearance pathways in aging Alzheimer's disease mice. J. Neurosci. 28, 8354–8360.

Hollingworth, P., Harold, D., Sims, R., Gerrish, A., Lambert, J.C., Carrasquillo, M.M., Abraham, R., Hamshere, M.L., Pahwa, J.S., Moskvina, V., et al., 2011. Common variants at ABCA7, MS4A6A/MS4A4E, EPHA1, CD33 and CD2AP are associated with Alzheimer's disease. Nat. Genet. 43, 429–435.

Huang, Y., Mucke, L., 2012. Alzheimer mechanisms and therapeutic strategies. Cell 148, 1204–1222.

Iliuk, A.B., Martin, V.A., Alicie, B.M., Geahlen, R.L., Tao, W.A., 2010. In-depth analyses of kinase-dependent tyrosine phosphoproteomes based on metal ion-functionalized soluble nanopolymers. Mol. Cell. Proteomics 9, 2162–2172.

Jay, T.R., Miller, C.M., Cheng, P.J., Graham, L.C., Bemiller, S., Broihier, M.L., Xu, G., Margevicius, D., Karlo, J.C., Sousa, G.L., Cotleur, A.C., Butovsky, O., Bekris, L., Staugaitis, S.M., Leverenz, J.B., Pimplikar, S.W., Landreth, G.E., Howell, G.R., Ransohoff, R.M., Lamb, B.T., 2015. TREM2 deficiency eliminates TREM2+ inflammatory macrophages and ameliorates pathology in Alzheimer's disease mouse models. J. Exp. Med. 212, 287–295.

Jekabsone, A., Mander, P.K., Tickler, A., Sharpe, M., Brown, G.C., 2006. Fibrillar beta-amyloid peptide Abeta1-40 activates microglial proliferation via stimulating TNF-alpha release and H_2O_2 derived from nadph oxidase: a cell culture study. J. Neuroinflammation 3, 24.

Jonsson, T., Stefansson, H., Steinberg, S., Jonsdottir, I., Jonsson, P.V., Snaedal, J., Bjornsson, S., Huttenlocher, J., Levey, A.I., Lah, J.J., Rujescu, D., Hampel, H., Giegling, I., Andreassen, O.A., Engedal, K., Ulstein, I., Djurovic, S., Ibrahim-Verbaas, C., Hofman, A., Ikram, M.A., van Duijn, C.M., Thorsteinsdottir, U., Kong, A., Stefansson, K., 2013. Variant of TREM2 associated with the risk of Alzheimer's disease. N. Engl. J. Med. 368, 107–116.

Keshvara, L.M., Isaacson, C.C., Yankee, T.M., Sarac, R., Harrison, M.L., Geahlen, R.L., 1998. SYK- and Lyn-dependent phosphorylation of SYK on multiple tyrosines following B cell activation includes a site that negatively regulates signaling. J. Immunol. 161, 5276–5283.

Kiefer, F., Brumell, J., Al-Alawi, N., Latour, S., Cheng, A., Veillette, A., Grinstein, S., Pawson, T., 1998. The SYK protein tyrosine kinase is essential for Fcγ receptor signaling in macrophages and neutrophils. Mol. Cell. Biol. 18, 4209–4220.

King, O.D., Gitler, A.D., Shorter, J., 2012. The tip of the iceberg: RNA-binding proteins with prion-like Domains in neurodegenerative disease. Brain Res. 1462, 61–80.

Koppers, M., van Blitterswijk, M.M., Vlam, L., Rowicka, P.A., van Vught, P.W., Groen, E.J., Spliet, W.G., Engelen-Lee, J., Schelhaas, H.J., de Visser, M., van der Kooi, A.J., van der Pol, W.L., Pasterkamp, R.J., Veldink, J.H., van den Berg, L.H., 2012. VCP mutations in familial and sporadic amyotrophic lateral sclerosis. Neurobiol. Aging 837, e7–e13.

Krabbe, G., Halle, A., Matyash, V., Rinnenthal, J.L., Eom, G.D., Bernhardt, U., Miller, K.R., Prokop, S., Kettenmann, H., Heppner, F.L., 2013. Functional impairment of microglia coincides with beta-amyloid deposition in mice with alzheimer-like pathology. PLoS One 8, e60921.

Krisenko, M.O., Higgins, R.L., Ghosh, S., Zhou, Q., Trybula, J.S., Wang, W.-H., Geahlen, R.L., 2015. Syk is recruited to stress granules and promotes their clearance through autophagy. J. Biol. Chem. (in press).

Lee, J.K., Tansey, M.G., 2013. Microglia isolation from adult mouse brain. Methods Mol. Biol. 1041, 17–23.

Linnartz, B., Wang, Y., Neumann, H., 2010. Microglial immunoreceptor tyrosine-based activation and inhibition motif signaling in neuroinflammation. Int. J. Alzheimers Dis. 2010, 587463.

Liu-Yesucevitz, L., Bilgutay, A., Zhang, Y.J., Vanderweyde, T., Citro, A., Mehta, T., Zaarur, N., McKee, A., Bowser, R., Sherman, M., Petrucelli, L., Wolozin, B., 2010. Tar DNA binding protein-43 (TDP-43) associates with stress granules: analysis of cultured cells and pathological brain tissue. PLoS One 5, e13250.

Loeffler, D.A., 2013. Intravenous immunoglobulin and Alzheimer's disease: what now? J. Neuroinflammation 10, 70.

McDonald, D.R., Bruden, K.R., Landreth, G.E., 1997. Amyloid fibrils activate tyrosine kinase-dependent signaling and superoxide production in microglia. J. Neurosci. 17, 2284–2294.

McEwen, E., Kedersha, N., Song, B., Scheuner, D., Gilks, N., Han, A., Chen, J.-J., Anderson, P., Kaufman, R.J., 2005. Heme-regulated inhibitor kinase-mediated phosphorylation of eukaryotic translation initiation factor 2 inhibits translation, induces stress granule formation, and mediates survival upon arsenite exposure. J. Biol. Chem. 280, 16925–16933.

Menzies, F.M., Fleming, A., Rubinsztein, D.C., 2015. Compromised autophagy and neurodegenerative diseases. Nat. Rev. Neurosci. 16, 345–357.

Meyer-Luehmann, M., Spires-Jones, T.L., Prada, C., Garcia-Alloza, M., De Calignon, A., Rozkalne, A., Koenigsknecht-Talboo, J., Holtzman, D.M., Bacskai, B.J., Hyman, B.T., 2008. Rapid appearance and local toxicity of amyloid-beta plaques in a mouse model of Alzheimer's disease. Nature 451, 720–724.

Miller, Y.I., Choi, S.H., Wiesner, P., Bae, Y.S., 2012. The SYK side of TLR4: signalling mechanisms in response to LPS and minimally oxidized LDL. Br. J. Pharmacol. 167, 990–999.

Mócsai, A., Abram, C.L., Jakus, Z., Hu, Y., Lanier, L.L., Lowell, C.A., 2006. Integrin signaling in neurtrophils and macrophages uses adaptors containing immunoreceptor tyrosine-based activation motifs. Nat. Immunol. 7, 1326–1333.

Mosher, K.I., Wyss-Coray, T., 2014. Microglial dysfunction in brain aging and Alzheimer's disease. Biochem. Pharmacol. 88, 594–604.

Moussaud, S., Draheim, H.J., 2010. A new method to isolate microglia from adult mice and culture them for an Extended period of time. J. Neurosci. Methods 187, 243–253.

Naj, A.C., Jun, G., Beecham, G.W., Wang, L.S., Vardarajan, B.N., Buros, J., Gallins, P.J., Buxbaum, J.D., Jarvik, G.P., Crane, P.K., et al., 2011. Common variants at MS4A4/MS4A6E, CD2AP, CD33 and EPHA1 are associated with late-onset Alzheimer's disease. Nat. Genet. 43, 436–441.

N'Diaye, E.N., Branda, C.S., Branda, S.S., Nevarez, L., Colonna, M., Lowell, C., Hamerman, J.A., Seaman, W.E., 2009. TREM-2 (triggering receptor expressed on myeloid cells 2) is a phagocytic receptor for bacteria. J. Cell Biol. 184, 215–223.

Neumann, M., Sampathu, D.M., Kwong, L.K., Truax, A.C., Micsenyi, M.C., Chou, T.T., Bruce, J., Schuck, T., Grossman, M., Clark, C.M., McCluskey, L.F., Miller, B.L., Masliah, E., Mackenzie, I.R., Feldman, H., Feiden, W., Kretzschmar, H.A., Trojanowski, J.Q., Lee, V.M., 2006. Ubiquitinated TDP-43 in frontotemporal lobar degeneration and amyotrophic lateral sclerosis. Science 314, 130–133.

Pan, X.D., Zhu, Y.G., Lin, N., Zhang, J., Ye, Q.Y., Huang, H.P., Chen, X.C., 2011. Microglial phagocytosis induced by fibrillar beta-amyloid is attenuated by oligomeric beta-amyloid: implications for Alzheimer's disease. Mol. Neurodegener. 6, 45.

Paris, D., Ait-Ghezala, G., Bachmeier, C., Laco, G., Beaulieu-Abdelahad, D., Lin, Y., Jin, C., Crawford, G., Mullan, M., 2014. The spleen tyrosine kinase (Syk) regulates alzheimer amyloid-β production and Tau hyperphosphorylation. J. Biol. Chem. 289, 33927–33944.

Perry, G., Cash, A.D., Smith, M.A., 2002. Alzheimer disease and oxidative stress. J. Biomed. Biotechnol. 2, 120–123.

Relkin, N.R., Szabo, P., Adamiak, B., Burgut, T., Monthe, C., Lent, R.W., Younkin, S., Younkin, L., Schiff, R., Weksler, M.E., 2009. 18-Month study of intravenous immunoglobulin for treatment of mild Alzheimer disease. Neurobiol. Aging 30, 1728–1736.

Righi, M., Mori, L., De Libero, G., Sironi, M., Biondi, A., Mantovani, A., Donini, S.D., Ricciardi-Castognoii, P., 1989. Monokine production by microglial cell clones. Eur. J. Immunol. 19, 1443–1448.

Schieven, G.L., Kirihara, J.M., Burg, D.L., Geahlen, R.L., Ledbetter, J.A., 1993. p72SYK tyrosine kinase is activated by oxidizing conditions that induce lymphocyte tyrosine phosphorylation and Ca^{2+} signals. J. Biol. Chem. 268, 16688–16692.

Solito, E., Sastre, M., 2012. Microglia function in Alzheimer's disease. Front. Pharmacol. 3, 14. http://dx.doi.org/10.3389/fphar.2012.00014.

Sondag, C.M., Dhawan, G., Combs, C.K., 2009. Beta amyloid oligomers and fibrils stimulate differential activation of primary microglia. J. Neuroinflammation 6, 1. http://dx.doi.org/10.1186/1742-2094-6-1.

Sudduth, T.L., Greenstein, A., Wilcock, D.M., 2013. Intracranial Injection of Gammagard, a human IVIg, modulates the inflammatory response of the brain and lowers Aβ in APP/PS1 mice along a different time course than anti-Aβ antibodies. Neurobiol. Dis. 33, 9684–9692.

Takahashi, K., Rochford, C.D., Neumann, H., 2005. Clearance of apoptotic neurons without inflammation by microglial triggering receptor expressed on myeloid cells-2. J. Exp. Med. 201, 647–657.

Turner, M., Mee, P.J., Costello, P.S., Williams, O., Price, A.A., Duddy, L.P., Furlong, M.T., Geahlen, R.L., Tybulewicz, V.L.J., 1995. Perinatal lethality and a block in the development of B Cells in mice lacking the tyrosine kinase p72SYK. Nature 378, 298–302.

Uy, B., McGlashan, S.R., Shaikh, S.B., 2011. Measurement of reactive oxygen species in the culture media using Acridan Lumigen PS-3 assay. J. Biomol. Tech. 22, 95–107.

Vanderweyde, T., Yu, H., Varnum, M., Liu-Yesucevitz, L., Citro, A., Ikezu, T., Duff, K., Wolozin, B., 2012. Contrasting pathology of the stress granule proteins TIA-1 and G3BP in tauopathies. J. Neurosci. 32, 8270–8283.

Vlad, S.C., Miller, D.R., Kowall, N.W., Felson, D.T., 2008. Protective effects of NSAIDs on the development of Alzheimer disease. Neurology 70, 1672–1677.

Waelter, S., Boeddrich, A., Lurz, R., Scherzinger, E., Lueder, G., Lehrach, H., Wanker, E.E., 2001. Accumulation of mutant huntingtin fragments in aggresome-like inclusion bodies as a result of insufficient protein degradation. Mol. Biol. Cell 12, 1393–1407.

Wang, W.-H., Childress, M.O., Geahlen, R.L., 2014. SYK interacts with and phosphorylates nucleolin to stabilize Bcl-xL mRNA and promote cell survival. Mol. Cell. Biol. 34, 3788–3799.

Wang, Y., Cella, M., Mallinson, K., Ulrich, J.D., Young, K.L., Robinette, M.L., Gilfillan, S., Krishnan, G.M., Sudhakar, S., Zinselmeyer, B.H., Holtzman, D.M., Cirrito, J.R., Colonna, M., 2015. TREM2 lipid sensing sustains the microglial response in an Alzheimer's disease Model. Cell 160, 1061–1071.

Xue, L., Wang, W.-H., Iliuk, A., Hu, L., Galan, J.A., Yu, S., Hans, M., Geahlen, R.L., Tao, W.A., 2012. Sensitive kinase assay linked with phosphoproteomics for identifying direct kinase substrates. Proc. Natl. Acad. Sci. U. S. A. 109, 5615–5620.

Yi, Y.S., Son, Y.-J., Ryou, C., Sung, G.-H., Kim, J.-H., Cho, J.Y., 2014. Functional roles of SYK in macrophage-mediated inflammatory responses. Mediat. Inflamm. 2014, 270302.

Zhang, B., Gaiteri, C., Bodea, L.G., Wang, Z., McElwee, J., Podtelezhnikov, A., Zhang, C., Xie, T., Tran, L., Dobrin, R., Fluder, E., Clurman, B., Melquist, S., Narayanan, M., Suver, C., Shah, H., Mahajan, M., Gillis, T., Mysore, J., MacDonald, M.E., Lamb, J.R., Bennett, D.A., Molony, C., Stone, D.J., Gudnason, V., Myers, A.J., Schadt, E.E., Neumann, H., Zhu, J., Emilsson, V., 2013. Integrated systems approach identifies genetic nodes and networks in late-onset Alzheimer's disease. Cell 153, 707–720.